**A petrographic study of the anthropomorphic stelae from the Megalithic Area of Saint-Martin-de-Corléans (Aosta, Northern Italy),**



*Published version:*

DOI:10.1111/arcm.12053

# A petrographic study of the anthropomorphic stelae from the Megalithic Area of Saint-Martin-de-Corléans (Aosta, Northern Italy)

Rubinetto V.[1], Appolonia L.[2], De Leo S.[2], Serra M.[†], Borghi A.[1]

[1] Dipartimento di Scienze della Terra – Università degli Studi di Torino

[2] Soprintendenza per i Beni e le Attività Culturali della Regione autonoma della Valle d'Aosta

## Abstract

The Megalithic Area of Saint-Martin-de-Corléans consists of anthropomorphic stelae dated at the Copper Age and at the beginning of the Ancient Bronze Age. They were curved in different lithologies of various provenance according to two successive artistic styles, “ancient” and “evolved”.

A minero-chemical and petrographic investigation were carried out on 47 stelae and on reference samples collected from 8 different outcrops aimed to define the provenance of the stone materials. The variety of rocks used for the realization of the stelae reflects the geologic complexity of Aosta Valley.

Most of the examined stelae were classified as foliated impure marbles, gray banded marbles (Bardiglio), calcschists and metabasites belonging to the Upper Piedmont Zone, which outcrops in close proximity of the Megalithic Area. Some stelae of the evolved group consisted of massive marbles with silicate layers attributed to the Sion-Courmayeur zone. Similar stone materials were reported for the stelae of the same age found at the archaeological area of Petit Chasseur (Sion, Switzerland). It can be interpreted as the materic attestation of the archaeological affinity between the stelae occurring in the two pre-historic sites, supporting the hypothesis of cultural exchanges over the Grand St. Bernard Pass since the Early Copper Age.

## Key words

Anthropomorphic stelae, petrographic analysis, provenance study, Copper age, Aosta Valley (NW Italy), Western Alps

## Introduction

The Megalithic Area of Saint-Martin-de-Corléans consists of a pre-historic anthropomorphic stelae site uncovered in 1969 (Mezzena, 1978). It is located in the western outskirts of the city of Aosta (North-western Italy), on the alluvial sediments of Dora Baltea river and extends over an area of one hectare.

The stratified deposit testifies a long anthropological evolution of the area, by the end of Neolithic period to the Iron and Roman Ages, but the most important documentation is referred to the megalithic monuments, stelae and tombs of the Copper Age and the beginning of the Ancient Bronze Age.

Based on archaeological research, it was possible to divide the history of the site, which remained active as an area of worship and burial for almost a millennium, from about 3000 BC to 1900 BC, into five chronological stages (Mezzena, 1998). The earliest phase corresponds to an alignment of 22 large cylindrical wooden poles oriented from northeast to southwest. With the second phase, dating between 2750 BC and 2400 BC, the area of the cult acquires more importance, conferred by the construction of two orthogonal alignments of more than 45 anthropomorphic stelae developed along two orthogonal axes, respectively oriented to northeast-southwest and northwest-southeast, maintaining the schedule followed for the installation of poles and plowing. The stelae, about two - three meters high and one meter wide, with thicknesses of few tens of centimeters, consist of various lithologies, characterized by different workability in term of ways and finishes (De Leo, 2006). The stelae were carved according to two successive artistic styles, named “ancient”, with representations of clothing and anthropomorphic attributes reduced to essentials, and “evolved”, showing a more complex and detailed representation (Fig. 1). All the stelae, the ancient ones and the most recent too, are similar to those of the Petit Chasseur archaeological site near Sion (Switzerland), in respect of whom had been related by common features in terms of style and iconography (Bornaz *et al*., 2007). In the third phase, platforms associated with the stelae were built using plates and pebbles. They may be connected with ancient rituals, in fact an array of cylindrical wells, inside of which seeds of wheat and millstones have been found, was interpreted as ritual by farmers and growers of cereals.

Later, around 2300 BC, the site, originally attended for purposes of worship, also became burial area, as large tomb structures, defined "megalithic” for this reason, were constructed. In particular, during the fourth chronological phase, five tombs of various types were erected in different zones of the site. During this stage, a systematic re-use of the anthropomorphic stelae, taken by their early arrangement and used for the construction of different types of megalithic tombs, occurred. The systematic reuse of anthropomorphic stelae also continued under the fifth phase (2100-1800 BC), during which other three megalithic tombs were built. At the beginning of the Ancient Bronze Age, the cycle of the worship and burial area is concluded. Despite this, although the kind of evidences are not specified yet, it is not certain that the area was completely abandoned, since Iron Age and Roman Age levels were found.

The frequent reuse of the stelae, together with the complexity of geology of the Aosta Valley, requires a detailed study in order to classify them on the basis of archaeometric parameters and to define the provenance of the stones used for their realization.

Though these stelae were studied in detail from an archaeological point of view (Mezzena, 1978; 1998), as well as their significant historical value, no archaeometric approach had been undertaken so far for their scientific characterization. It would provide the necessary tools to restorers and archaeologists to carry out targeted conservation actions on the basis of future exposure aimed at an upcoming museum placement. For this reason, a research program in common with the Cultural Heritage and Activities Office of the self-governing Region of Aosta Valley was recently developed, and this led to some first preliminary results (Appolonia *et al.*, 2010; Serra *et al.*, 2012). This article presents a complete mineralogical and petrographic study, with the aim to define the geological nature of the stele and to provide information about the origin of the raw materials on the basis of a comparison between selected fragments of the stelae and samples coming from abandoned quarries of marbles outcropping along the Aosta Valley. In Table 1 A and B a comparison between stelae and representative quarries samples for lithology and modal compositions was reported.



**Geological Setting**

From a geological point of view, the archaeological site of Saint-Martin-de-Corléans is located within the external ophiolitic unit of the Combin Zone (Bigi *et al.*, 1990; Bonetto *et al.*, 2010), recently named Aouilletta unit (Malusà, 2004; Malusà *et al.*, 2005) (Fig. 2) and represents the relics of the Mesozoic Piedmont-Ligurian ocean separating the European and Insubric continental margins (e.g. Dal Piaz, 1999; Beltrando *et al.*, 2010 and refs therein).

As a result of the Alpine orogeny, the Piedmont Zone consists of several tectonic units, recording a polyphasic metamorphic history. These tectonic units may be distinguished into two tectono-metamorphic groups of ophiolitic units according to their tectonic positions, lithological association and contrasting metamorphic imprint. The Lower Piedmont Unit (Zermatt-Saas) disappears under the Mischabel and Gran Nomenon backfolds and it is dominated by metamorphic ophiolites derived from oceanic mafic and ultramafic protoliths and characterized by an eclogitic imprint of Eocene age and a subsequent retrogression toward greenschist facies conditions (Ernst and Dal Piaz, 1978; Dal Piaz *et al.*, 2001; Angiboust *et al.*, 2009; Beltrando *et al.*, 2010). The upper part of the Piedmont nappe stack (Combin Zone) mainly consists of Mesozoic metasediments (carbonaceous to terrigenous calcschists and impure marbles) alternating with tabular beds of greenschist facies tholeiitic metabasalts (named prasinites) and including lenses, in places very large, of serpentinites and minor metagabbros (Aouilletta unit); relics of sodic amphiboles and losange-shaped pseudomorphs after lawsonite document the existence of a blueschist facies event (no isotope dating) before the pervasive greenschist facies overprint of late Eocene-early Oligocene age (Caby, 1981; Baldelli *et al.,* 1983; Sartori, 1987; Marthaler and Stampfli, 1989; Burri *et al.,* 1998; Dal Piaz, 1999; De Giusti *et al.,* 2004; Malusà, 2004; Dal Piaz *et al.,* 2010).

Exotic sheets of continental origin discontinuously occur near the base of the Upper Piedmont Zone (Combin), both in the southern (*Fascio di Cogne*; Elter, 1971, 1972) and northern side (Pancherot-Cime Bianche unit; Dal Piaz, 1999, and refs therein) of the Aosta Valley. These tectonic sheets consist of Permian silvery quartzitic schists, Eotriassic tabular quartzites followed by dolostones and marbles (Middle-Late Triassic), slope breccias with dolomite fragments (Juras ) and basinal marbles and ophiolite free calcschists (Cretaceous ?).

In proximity to the investigated area, there are also other relevant geological units of the Alpine chain (Fig. 2). They consist of several varieties of continental crust rocks distinguished on the basis of their different metamorphic equilibration and paleogeographic provenance, such as the Monte Emilius Klippe (equlilibrated under eclogitic facies conditions); the Dent Blanche and the Mont Mary nappes (greenschists facies conditions), the Gran Paradiso Massif (eclogitic facies conditions), the Grand St. Bernard Nappe (blueschist facies conditions) and the Houillére Zone (greenschists facies conditions). They mainly consists of  mono and poly-metamorphic silicate-bearing rocks as micaschists and orthogneisses and minor meta-carbonatic cover of Mesozoic age (e.g. Govi, 1975; De Giusti *et al.*, 2004; Malusà *et al.*, 2005). Finally, in the more external position of the Penninic domain the Sion – Courmayeur Zone outcrops (Elter and Elter, 1965), interpreted as an outer oceanic unit respect to the Piedmont Zone (Loprieno *et al.*, 2011,and refs therein ).

In Aosta Valley, the Sion – Courmayeur Zone consists of two main geological units: the Roignais Versoyen Unit and the Bréches de Tarensaise Unit. The first is composed of oceanic metasediments, metabasites and serpentinitized lherzolites of Mesozoic age. The presence in the metabasites of high-pressure metamorphic assemblages is reported (Cannic *et al.*, 1996; Beltrando *et al.*, 2010;  and refs therein). The Brèches de Tarentaise (or Valais flysch)  are composed by the following succession from bottom to top: the Couches de l'Aroley, the Couches de Marmontains and the Couches de Saint-Christophe (Antoine, 1972; Fudral, 1973). The age of the Brèches de Tarentaise is still debated, it could be Senonian to Campanian (Antoine, 1972) or Priabonian (Gely, 1989). They mainly consists of carbonate and pelitic metasediment with bodies of polygenic breccias and are interpreted as a high pressure metamorphosed flysch deposited in the oceanic trench during Alpine convergence (Loprieno *et al.*, 2011

**Sampling and Analytical methods**

The petrographic characterisation was performed through 30 reference samples collected in 8 different outcrops within Aosta Valley (Fig. 2). They were compared with 55 samples belonging to 47 stelae, , collected during the recent restoration (Tables 1A and 1B). The samples, of a few cubic centimetres, were cut from the fresh fractured side of each single stelae and were used for preparing thin sections for petrological examination. Samples were analyzed coupling optical microscopy and scanning electron microscopy (Cambridge Stereoscan S360). An Energy Dispersive X-Ray Spectrometer (EDS) equipped with a pentafet detector (Oxford Instruments) was used to determine the chemical composition of the most discriminative minerals. Natural oxides and silicates (Astimex Scientific Limited) were acquired as standards. Acceleration current was set at 15 kV and counting time was 60 s. A ZAF data reduction program was used. All the analyses were recalculated using the MINSORT computer program of Petrakakis and Dietrich (1985). The mineral compositions are expressed as atoms per formula unit (a.p.f.u.). The mineral symbols are from Kretz (1983).

The petrographic analysis was carried out to define the mineralogical assemblage and the microstructural features of different material stone variety. The electron microprobe analysis has provided the chemical composition of the main mineral component and the chemical composition of accessory minerals useful for discriminative purposes. Locations of analysed samples are shown in Fig. 2 while representative compositions of minerals are reported in Tables 2, 3, and 4.

## Results

### Petrographic features

Most of the stelae show different varieties of very similar marble, difficult to distinguish from each other by a simple macroscopic observation.

Based on structural, paragenetic and compositional parameters, the large group of carbonate rocks can be divided into four main lithological varieties characterized by homogeneous metamorphic and structural features. In detail, the following lithological types have been distinguished: 1) foliated impure marbles, 2) calcschists, 3) gray banded marbles, locally named "Bardiglio", 4) massive marbles with silicate layers. As regards the composition of silicate-bearing rocks, metabasites from submarine basalts (prasinites), micaschists, orthogneisses and quartzites were observed. In only one case a sedimentary rock was found, represented by a travertine sample. Fig. 3 shows a quantitative distribution of the different lithologies identified among the stelae analyzed.

Foliated impure marbles and calcschists

The most abundant materials belong to a wide class consisting of foliated impure marbles and calcschists coming from the Combin Zone (Table 1A).

This class of rocks is characterized by the following metamorphic mineral assemblage: calcite (40-80 vol. % ), ankerite (5-10 vol.%), quartz (5-40 vol. %), white micas (muscovite and paragonite) (5-25 vol. %), Mg-chlorite (0-10 vol. %), clinozoisite (<5 vol.%), albite (0-10 vol. %), graphite (<5 vol. %). The accessories are rutile, titanite, apatite, zircon, tourmaline, iron sulphides and iron oxides. From a structural point of view these marbles show a medium to fine grained size, a foliated texture defined by alternating thin layers of white mica and the silicates cited above with more powerful domains of oriented xenoblastic calcite (Fig. 4A). Quartz domains and pseudomorphs after lawsonite consisting of graphite, calcite and paragonite also occur (Fig. 4B).

Gray banded marbles (Bardiglio)

Among the different varieties of marble occurring for the stelae production, it follows the gray banded marble coming from the ancient mining site located near the villages of Aymavilles, Saint Pierre e Villeneuve (Fig. 2). This marble, locally termed "Bardiglio" and also known by ancient Romans, is characterized by a regular alternation of centimeter-scale dark gray layers, consisting of calcite and dolomite, with levels of lighter gray tonality, where calcite only occurs (Fig. 5A). Microscopically this marble is easily distinguishable, for the presence of fine-grained dolomite layers alternating with calcitic ones (80-95 vol.%), as well as for the frequent occurrence of pseudomorphs after lawsonite, where the three compositional varieties of di-octahaedral micas are present (0-10 vol.%): muscovite, margarite and paragonite (Borghi *et al.*, 2006). The characteristic paragenesis of this marble is completed by the presence of albite, quartz, Mg-chlorite and phlogopite, pure magnesium end-member of biotitic mica (Fig. 4C). The accessories are rutile, titanite, apatite, zircon, tourmaline, graphite, iron sulphides and iron oxides.

Massive marbles with silicate layers

Nine of the analyzed samples (stelae 4 South, stelae 5, stelae 6, stelae 18, stelae 25, stelae 30, stelae 40, the roof of the tomb II, the interface between the stelae 6 south and the stelae 4 south) consist of centimeter levels marble alternating with foliated micaceous levels (massive marbles with silicate layers in Table 1A, Fig. 5B). This marble was used for the realization of the evolved style stelae, showing the most aesthetically refined decorations. It is microscopically characterized by a medium to fine grained size, a granoblastic structure and a planar preferred orientation of mica. In the carbonate matrix, quartz is present as isolated granoblasts and poikilitic porphyroblasts of albite occur (Fig. 4D). The main mineralogical association is composed of calcite (40-80 vol.%), quartz (10-40 vol.%), white mica (10-40 vol.%), Mg-chlorite (0-10 vol.%), clinozoisite (0-10 vol.%), albite (0-10 vol.%), graphite (<5 vol.%).. The accessories are rutile, titanite, apatite, zircon, tourmaline, iron sulphides and iron oxides. Sporadically, pseudomorphs after lawsonite to zoisite + white mica + quartz, amphibole and skeletal garnet crystals are also present (Fig. 4E).

### Silicate rocks

Finally, some stelae consist of silicate-bearing rocks. Particularly noteworthy is a variety of metabasite, named “prasinite”, used for stelae 9, stelae A, stelae P.

Prasinite consists of a metamorphic rock with a basic composition and represents the low-grade metamorphic product of original submarine basalt intercalations in the meta-sediments (calcschists) of the Upper Piedmont Zone. Their typical paragenesis is composed of calcium and sodium-calcium amphiboles (10-50 vol.%), epidote (10-35 vol.%), chlorite (0-10 vol.%), white mica (0-10 vol.%), biotite (0-10 vol.%) and albite (5-30 vol.%) (Fig. 4F). Quartz (5-10 vol.%) and, to accessory amount, rutile, titanite, garnet andiron oxides can also be present. They show a structure from massive to moderately schistose, with the presence of typical white albite porphyroblasts.

Stelae 11 and 20 (Table 1B) were found to consist of an orthogneiss with predominantly quartz (40-70 vol.%), potassium feldspar (10-40 vol.%), plagioclase (5-10 vol.%), white mica (5-10 vol.%), biotite (5-10 vol.%) and chlorite (<5 vol.%). Among the accessories, epidote, titanite, zircon, garnet and iron oxides prevail. This rock shows a characteristic milonitic texture defined by quartz - feldspar layers alternate with thin mica layers that underline the schistosity of the rock (Fig. 4G). Porphyroclasts relicts of magmatic potassium feldspar occur, and the original sites of magmatic plagioclase are also replaced by white mica and very fine-grained epidote felts. Finally, intensely brown pleochroic biotite has been found.

### Travertine

Only one of the samples can be classified as a micaschist of the crystalline basement units, which corresponds to the great slab in the passage between the tomb V and the tomb VII. The analyzed sample is a garnet micaschist, showing a millimeter to centimeter schistosity, consisting of quartz (35 vol.%), white mica (40 vol.%), albite (20 vol.%), chlorite (<5 vol.%), epidote (<5 vol.%)garnet and iron oxides. For the South-West pillar of the tomb II and for the North-East one of the tomb VII instead a fine-grained gneiss was observed. This rock, characterized by a foliated structure with crenulation, that suggest an albitic micaschist origin, consists of quartz (30-40 vol.%), white mica (20-40 vol.%), albite (20-30 vol.%) and Mg-Fe chlorite (<5 vol.%) and, as accessories, zircon and iron oxides.

Stelae 17 consists of a stilpnomelane-bearing quartzite (Fig. 4H). The rock is characterized by an isotropic and granoblastic texture and by a medium-grain size. It results to be formed predominantly of quartz (75% vol.), that occurs in equidimensional crystals without orientation, index of static recrystallization. There are also stilpnomelane (> 20% vol.), recognizable by the acicular shape, isolated crystals of white mica, chlorite, albite and accessory minerals such as tourmaline and iron oxides.

Finally, the north-west pillar of the Tomb V was found to be composed of travertine showing vacuolar structure and including quartz, mica, zoisite-clinozoisite and albite. The presence of metamorphic minerals in the carbonate matrix of the travertine implies a regional origin respect to a provenance from the travertine quarries of the central Italy, where metamorphic rock minerals are not reported. Travertine deposits are well-known and widespread in many places in the Aosta Valley. Rock formations of this type are present in the area to the north of Aosta (Bibian) or near Gressan along the right bank of the Dora Baltea river.

**Mineral Chemistry of the marble varieties**

Foliated impure marbles and calcschists

Based on the electron microprobe it was possible to distinguish in these rocks a potassium mica, characterized by high Si content (phengitic in composition) and a sodium mica (paragonite). Potassium mica shows a strong zoning characterized by a compositional change in Si content between 6.30 and 7.20 atoms per formula unit (a.p.f.u.) on the basis of 22 Ox. (Fig. 6A). This implies that the mica has grown under metamorphic conditions of high pressure, typical for the Combin Zone (e.g. Cartwright and Barnicoat, 2002). Moreover, K is partially replaced by Na with Na / (Na + K) ratio increasing, accompanied by the decrease of Si content in the composition of micas.

In turn, the calcschists chlorite is an intermediate variety between ripidolite and picnoclorite, while chlorite of foliated impure marbles plots in the ripidolite field, with a $Fe_{tot}$ / (Mg + $Fe_{tot}$) ratio ranging between 0.15 and 0.35 a.p.f.u. (Fig. 6B).

Gray banded marbles (Bardiglio)

The di-octahaedral micas of the gray banded marble (potassium mica) resulted phengitic in composition, with Si content ranging between 7.00 and 7.50 a.p.f.u. and characterized by a partial replacement of K by Na (Fig. 6C). Chlorite for this marble is found to be clinochlore in composition (Fig. 6D).

Massive marbles with silicate layers

Potassium mica shows a compositional zoning defined by the Si content ranging between 6.30 and 7.30 a.p.f.u., reflecting again a phengitic composition typical of rocks re-crystallized under high pressure metamorphic conditions (Fig. 6E). Chlorite for this marble is found to be ripidolite in composition (Fig. 6F).

The amphibole, only encountered in the silicate layers of the stelae 40, is characterised by high values of Si ranging between 7.25 and 7.75 a.p.f.u. on the basis of 23 Ox, with $Mg/(Mg+Fe^{2+})$ ratio around 0.60, a $(Na)_{M4}$ minor than 0.30 a.p.f.u. and a very low $(Na+K)_{A}$ (minor than 0.10 a.pf.u.) that let identify an intermediate phase between actinolite and actinolite-hornblende, according to Leake (1987).

The uncommon garnet occurring inside this marble variety showed the following composition: Almandine 38%, Spessartine Pyrope 2% and Grossular 28%. Among metamorphic minerals, the compositional of garnet [$(Fe, Mg, Ca, Mn)_3\ Al_2\ Si_3\ O_{12}$] is a key piece of information in metamorphic petrology because the chemical zoning preserved in the garnet porphyroblasts potentially records the changes in the reaction history of the rock (Spear, 1989). In particular, the presence of a manganese-rich garnet implies metamorphic conditions of formation characterized by low values of temperature (<500 ° C) (Spear *et al.*, 1991), documented by the occurrence of lawsonite and other blueschist facies minerals and by the greenschist facies overprint, testified by actinolitic composition of the amphibole.

**Discussion**

Based on minero – petrographic data, the carbonate-bearing rocks (different varieties of marbles and calcschists) were found to be the 82% of the total rock constituting the anthropomorphic stelae (Fig. 3). This is justifiable since the average hardness of these rocks is lower than that of silicate rocks. This feature allows an easier workability by people with limited technological capabilities. Also as regards the geological framework of the site, carbonate rocks are locally more abundant than silicate rocks, which represent 18% of the rock types encountered.

As regards their site of provenance, most of the analyzed rock types (52%) are composed by impure foliated marbles and calcschists belonging to the Upper Piedmont Zone, which outcrops in the close proximities of the archaeological site.

Following the comparison of their features with samples collected in the field, this variety of marbles and calcschists resulted very similar from a mineralogical and structural point of view with samples coming from ancient quarry sites located near the Megalithic Area. Also minero-chemical data confirmed the good correlation with marbles and calcschists of the Combin Zone (Fig. 6A). In particular, white mica resulted compositionally similar to that found in samples collected near the marble outcropping in correspondence of Pont d'Avisod locality, along the gorge of the Clou Neuf stream, just a few hundred meters from the archaeological site (Fig. 2).

Even, the provenance of the prasinites has to be considered local, very close to the site of use. The prasinites, indeed, occur regularly interbedded with the calcschists. Given the spread diffusion near the archaeological area and the easy workability of this lithology, it is not surprising that it has been used mainly in the early stages of occupation of the site.

As for the Bardiglio gray banded marbles, a good correlation between the chemical composition of di-octahaedral micas belonging to samples from the site of the Pesse-Montbel quarry near Aymavilles village and those belonging to stelae samples, was detected (Fig. 2). The good mineralogical and compositional correlation between quarry samples and fragments of the stele suggests to attribute this marble variety to stelae 3 South, stelae 29, stelae 31 and to the NE pillar of Tomb II (Table 1A). The Bardiglio marble too belongs to the Upper Piedmont Zone. Particularly, it outcrops near the tectonic contact with the Grand St. Bernard Nappe, which occurs in the Aosta Valley in the outer position with respect to the Piedmont Zone at a dozen miles upstream of the archaeological site (Fig 2).

The stelae consisting of massive marble with silicate layers (4 south, 5, 6, 18, 25, 30, 40, the roof of the tomb II, the interface between the stelae 4 south and 6 south) differs significantly from those previously described. In particular, it does not appear to come from outcrops in the immediate vicinity of the megalithic site. Vice versa, this rock type shows mineralogical and petrographic features similar to marble varieties that outcrop in the Sion - Courmayeur Unit, especially with the variety historically known as the “Morgex Stone” and sampled at the Drumeilleux – and Liconi quarries in the Morgex municipality (Fig. 2).

Particularly noticeable in Fig. 6E is the good correlation between the chemical composition of the di-octahedral micas (muscovite and paragonite) of stelae and quarries samples. Even the representative analysis of chlorite shows a good compositional correlation between the samples collected in the quarries and those from the stelae, projecting both of them in the field of ripidolite (Fig 6F).

With regard to the sporadic presence of orthogneiss, micaschist, fine-grained gneiss and quartzite, despite these lithologies do not outcrop in the immediate vicinity of the archaeological site, they are well represented in the form of erratic blocks deposited by the glaciers of Quaternary Age on the flanks of the valley or at its mouth along the main axis of the Aosta valley.

In the case of orthogneisses, petrographic characters are very similar to those of the milonitic orthogneisses of the Arolla Series in the Dent Blanche Nappe (Pennacchioni and Guermani, 1993; Bucher *et al.*, 2004), which outcrops a few kilometres north-east of Aosta, along the Valpelline (Fig. 2). It is therefore likely that in this case it has been used a stone boulder carried by the Valpelline glacier near the archaeological site of Saint-Martin-de-Corléans. It should be noted that th[illegible]imilar rocks also occur within the basement units of the Gran St. Bernard nappe system (Gouffon, 1993; Sartori *et al.*, 2006).

Regard to the quartzite, the occurrence of stilpnomelane, a femic sheet-silicate similar to biotite, implies low-temperature metamorphic conditions in greenschist facies (Brown, 1971). Interbedded quartzites are common in metamorphic rocks outcropping in the Aosta Valley, especially in the Permian-Eotriassic succession of the Zone Houillére or other silicoclastic cover units of the Gran St. Bernard nappe system (Gouffon, 1993; Sartori *et al.*, 2006) in the Avise syncline (Dal Piaz and Govi, 1968) or in the Sion – Courmayeur Zone (Loprieno *et al.*, 2011). In this case it is therefore not possible to precisely identify the area of origin of this stone material, although the presence of stilpnomelane would suggest a low-grade metamorphic unit and thus an origin more external than the Piedmont Zone.

Finally, in the case of micaschists and fine-grained gneisses, it was probably the use of an erratic block found near the site and coming from one of the many metamorphic continental crust units outcropping upstream of the site.



**Conclusions**

A detailed characterization of the minero-petrographic rock types used in the production of the pre-historic stelae discovered in Saint-Martin-de-Corléans (Aosta, NW Italy) site allowed in most cases to define the area or at least the tectonometamorphic units of provenance of stone material.

In particular, combining archaeometric and archaeological data, it was noted that stelae of ancient style resulted carved using stone materials coming from areas located near the archaeological site, while stelae belonging to the stylistically more advanced period were manufactured by means of rocks outcropping more distant, as “Bardiglio” and “Morgex Stone” marbles. It is therefore likely that in the latter evolution phases of the site, corresponding to the Copper Age and the beginning of the Ancient Bronze Age, local residents developed contacts with neighbouring populations. In the specific case, for the stelae consisting of massive marble with silicate layers the original quarries were probably placed in the area near Morgex village, located at approximately 30 km from the Saint-Martin-de-Corléans archaeological site and belonging to the Sion – Courmayeur geological unit.

At this regard it should be pointed out that the Sion - Courmayeur geological unit continues north-east up to Sion, in Switzerland, where material stones similar to Morgex marbles were used for the realization of several anthropomorphic stelae found at the archaeological site of Petit Chasseur (Sartori *et al.*, 2007). These Authors inferred the provenance area of micaceous marbles used for the stelae production at the Pierre Avoi formation (Bagnoud *et al.*, 1998), outcropping on the right side of the Rhone river and corresponding for age and lithological association to the Brèches de Tarentaise. In relation to the Sion stelae, the apparent common characteristics with the Aosta stelae of evolved style, already observed in terms of stylistic and iconographic features (Bornaz *et al*., 2007), can also be now confirmed by the geologic and petrographic observations, supporting the hypothesis of cultural exchanges across the Grand St. Bernard Pass since the Early Copper Age.

**Acknowledgments**.

This work was financially supported by Ministero dell'Università e della Ricerca Scientifica e Tecnologica (M.U.R.S.T.).

This paper is devoted to the memory of Margherita Serra: an unforgettable PhD student and friend who early left us, leaving an indelible trail behind her.

**References**

Angiboust, S., Agard, P., Jolivet, L. and Beyssac, O., 2009, The Zermatt–Saas ophiolite: the largest (60-km wide) and deepest (c. 70–80 km) continuous slice of oceanic lithosphere detached from a subduction zone?, *Terra Nova*, **21**, 171-180.

Antoine, P., 1972, Le domaine pennique externe entre Bourg Saint-Maurice (Savoie) et la frontiére italo-suisse, *Ph. D. Thesis,* University of Grenoble, 367 pp., and *Géologie Alpine*, **48**, 5-40.

Apollonia, L., Borghi, A., De Leo, S., Rubinetto, V. and Serra, M., 2010, Studio minero-petrografico delle stele antropomorfe dell'area megalitica di Saint-Martin-de-Corléans ad Aosta, *Bollettino della Soprintendenza per i Beni e le Attività Culturali della Valle d'Aosta*, Regione Autonoma Valle d'Aosta, **7**, 183-190.

Bagnoud, A., Wernli, R. and Sartori, M., 1998, Découverte de foraminifères planctoniques paléogènes dans la zone de Sion-Courmayeur à Sion (Valais, Suisse), *Eclogae Geologicae Helvetiae*, **9**, 421-429.

Baldelli, C., Dal Piaz, G.V. and Polino, R., 1983, Le quarziti a manganese e cromo di Varenche-St. Barthàlemy, una sequenza di copertura oceanica delle falda Piemontese, *Ofioliti*, **8**, 207-221.

Beltrando, M., Rubatto, D. and Manatschal, G., 2009, Preservation of an ocean-continent transition zone in the eclogitic Piemonte unit: implications for the dynamics of orogens, *Alpine Workshop*, Cogne 2009, Abstr.

Beltrando, M., Compagnoni, R. and Lombardo, B., 2010, (Ultra-) High-pressure metamorphism and orogenesis: An Alpine perspective, *Gondwana Research*, **18**, 147-166 (doi:10.1016/j.gr.2010.01.009).

Bigi, G., Castellarin, A., Coli, M., Dal Piaz, G.V., Sartori, R., Scandone, P. and Vai, G.B., 1990, Structural Model of Italy 1:500.000, Sheet 1. *C.N.R., Progetto Geodinamica*, SELCA, Firenze.

Bonetto, F., Dal Piaz, G.V., De Giusti F, Massironi, M., Monopoli, B. and Schiavo, A., 2010, Carta geologica della Valle d'Aosta alla scala 1:100.000. *Regione Autonoma Valle d'Aosta, Dipartimento difesa del suolo e risorse idriche*, Tipografia Valdostana, Aosta, 23 pp.

Borghi, A., Fiora, L. and Zoja, A., 2006, The grey marble of Porta Praetoria (Aosta, Italy): a minero-petrographic characterisation and provenance determination, *Periodico di Mineralogia*, **LXXXVI**, 59-74.

Bornaz, L., Porporato, C., Rinaudo, F., De Gattis, G. and Focareta, R., 2007, 3D high accuracy survey and modelling of one of Aosta's anthropomorphic stelae. In: *XXI International CIPA Symposium (GRC), International archives of the photogrammetry, remote sensing and spatial information sciences,* Athens, **Vol. XXXVI**-5/C53, 176-181.

Brown, E.H., 1971, Phase relations of biotite and stilpnomelane in the greenschist facies, *Contributions to Mineralogy and Petrology*, **31**, 275-299.

Bucher, K., Dal Piaz, G.V., Oberhänsli, R., Gouffon, Y., Martinotti, G. and Polino, R., 2004, Blatt 1347-Matterhorn, Erleuterungen. Atlas géologique de la Suisse 1:25.000, *Service hydrologique et géologique National*, Berne, 73 pp.

Burri, M., Alliman, M., Chessex, R., Dal Piaz, G.V., Della Valle, G., Du Bois, L., Gouffon, Y., Guermani, A., Hagen, T., Krummenacher, D. and Looser, M.O., 1998, Feuille 1346 Chanrion, avec partie nord de la feuille 1366 Mont Vélan, et Notice explicative. Atlas géologique de la Suisse 1:25.000, *Service hydrologique et géologique National,* Berne, 79 pp.

Caby, R., 1981, Le Mesozoique de la zone du Combin en val d'Aosta (Alpes Graies): des domaines pennique, austroalpin et océanique, *Géologie Alpine*, **57**, 5-13.

Cannic, S., Lardeaux, J.M., Mugnier, J.L. and Hernandez, J., 1996, Tectono-metamorphic evolution of the Roignais-Versoyen Unit (Valaisan domain, France), *Eclogae Geologicae Helvetiae*, **89**, 321-343.

Capedri, S., Venturelli, G. and Photiades, A., 2004, Accessory minerals and $^{18}$O and $^{13}$C marbles from the Mediterranean area, *Journal of Cultural Heritage*, **5**, 27-47.

Cartwright, I. and Barnicoat, A.C., 2002, Petrology, geochronology, and tectonics of shear zones in the Zermatt-Saas and Combin zones of the Western Alps, *Journal of Metamorphic Geology*, **20**, 263-281.

Dal Piaz, G.V. and Govi, M., 1968, Lo stilpnomelano in Valle d'Aosta: nuovi ritrovamenti. *Bollettino della Società Geologica Italiana*, **87**, 91-108.

Dal Piaz, G.V., 1999, The Austroalpine-Piedmont nappe stack and the puzzle of Alpine Tethys, *Memorie di Scienze Geologiche*, **51/1**, 155-176.

Dal Piaz, G.V., Cortiana, G., Del Moro, A., Martin, S., Pennacchioni, G. and Tartarotti, P., 2001, Tertiary age and paleostructural inferences of the eclogitic imprint in the Austroalpine outliers and Zermatt-Saas ophiolite Western Alps, *International Journal of Earth Sciences*, **90**, 668-684.

Dal Piaz, G.V., Gianotti, F., Monopoli, B., Pennacchioni, G., Schiavo, A., Tartarotti, P., *Et Alii,* 2010, Foglio 091 Chatillon e note illustrative. *Carta Geologica d'Italia alla scala 1:50.000*, licenziati per la stampa nel 2007.

De Giusti, F., Dal Piaz, G.V., Massironi, M. and Schiavo, A., 2004, Carta geotettonica della Valle d'Aosta*, Memorie di Scienze Geologiche,* **55**, 129-149.

De Leo, S., 2006, Caratterizzazione petrografica dei materiali costituenti le stele antropomorfe dell'area megalitica di Saint-Martin-de-Corléans in Aosta (Néolithique). In: *XI Colloque International sur les alpes dans l'antiquité: La pierre in milieu alpine*, Champsec / Val de Bagnes / Valais-Suisse, 33-40.

Elter, G., 1971, Schistes Lustrees et ophiolites the la zone piemontaise entre Orco et Doire Baltee (Alpes Graies). Hypothèses sur l'origine des ophiolites, *Géologie Alpine*, **47**, 147-169.

Elter G., 1972, Contribution à la connaissance de briançonnais interne et de la bordure piemontaise dans les Alpes Graies nord-orientales, *Memorie Istituto di Geologia e Mineralogia, Università di. Padova,* **28**, 18 pp.

Elter, G., 1987, Carte géologique de la Vallée d'Aoste. Cartographie et impression SELCA, Firenze, in Dal Piaz G.V. (2001): Commemorazione di Giulio Elter. *Memorie di Scienze Geologiche*, **53**, 153-162.

Elter, G. and Elter, P., 1965, Carta geologica della regione del Piccolo S. Bernardo (versante italiano). Note illustrative. *Memorie Istituto Geologico Mineralogico Università di Padova*, **25**, 1–53.

Ernst, W.G. and Dal Piaz, G.V., 1978, Mineral parageneses of eclogitic rocks and related mafic schists of the Piemonte ophiolite nappe, Breuil-St. Jacques area, Italian Western Alps, *American Mineralogist,* **63**, 621-640.

Fudral, S., 1973, Contribution à l'étude de l'unité de Moûtiers entre le torrent du Cormet d'Aréches et le hameau des Chapieux. *Ph. D. Thesis,* University of Grenoble, 129 pp.

Gely, J.P., 1989, Stratigraphie, tectonique et métamorphisme comparés de part et d'autre du front pennique en Tarentaise (Alpes de Savoie, France). *Ph. D. Thesis,* University of Chambéry, 343 pp.

Gouffon, Y., 1993, Géologie de la nappe du Grand St. Bernard entre la Dore Baltée et la frontiére suisse (Vallée d'Aoste, Italie). *Mémoires de Géologie,* Lausanne, **12**, 147 pp.

Govi, M., 1975, Carta del Ricoprimento Gran San Bernardo tra il Paramont ed il Vallone di Vertosan (Alta Valle d'Aosta) al 1:30.000. *Litografia Artistica Cartografica*, Firenze.

Hey, M.H., 1954, A new review of chlorites, *Mineralogical Magazine*, **30**, 277-292.

Kretz, R., 1983, Symbols for rock-forming minerals*, American Mineralogist*, **68**, 277-279.

Leake, B.E., 1978, Nomenclature of Amphiboles, *Canadian Mineralogist*, **16**, 501-520.

Loprieno, A., Bousquet, R., Bucher, S., Ceriani, S., Dalla Torre, F.H., Fugenschuh, B. and Schmid, S.M., 2011, The Valais units in Savoy (France): a key area for understanding the palaeogeography and the tectonic evolution of the Western Alps, *International Journal of Earth Sciences*, **100**, 963-992.

Marthaler, M. and Stampfli, G.M., 1989, Les schistes lustrées a ophiolies de la nappe du Satè: an ancien prisme d'accretion issue de la merge active apulienne*, Schweizerische Mineralogische und Petrographische Mitteilungen*, **69**, 211-216.

Malusà, M.G., 2004, Post-metamorphic evolution of the Western Alps: kinematic constraints from a multidisciplinary approach (mesostructural analysis, fission track dating, fluid inclusion analysis), *Ph. D. Thesis,* University of Turin, 335 pp.

Malusà, G., Polino, R. and Martin, S., 2005, The Gran San Bernardo nappe in the Aosta valley (western Alps): a composite stack of distinct continental crust units, *Bulletin de la Société géologique de France,* **176/5**, 417-431.

Mezzena, F., 1978, Le stele antropomorfe dell'arco alpino. Considerazioni ed appunti. In: *L'arte preistorica dell'Italia Settentrionale, catalogo della mostra*, Verona, 49-59.

Mezzena, F., 1998, Le stele antropomorfe dell'area megalitica di Aosta. In: *A.A.V.V. – Dei di Pietra. La grande statuaria antropomorfa nell'Europa del III millennio a.C.*. Skira, Milano, 14-121.

Pennacchioni, G. and Guermani, A., 1993, The mylonites of the Austroalpine Dent Blanche nappe along the northwestern side of the Valpelline valley (Italian Western Alps). *Memorie di Scienze Geologiche*, **45**, 37-55.

Petrakakis, K. and Dietrich, H., 1985, MINSORT: A program for the processing and archivation of microprobe analyses of silicate and oxide minerals, *Neues Jahrbuch für Mineralogie*, Monatshefte, **8,** 379-384.

Sartori, M., 1987, Structure de la zone du Combin entre les Diablond et Zermatt (Valais). *Eclogae Geologicae Helvetiae*, **80**, 789-814.

Sartori, M., Gouffon, Y. and Marthaler, M., 2006, Harmonisation et définition des unités lithostratigraphiques briançonnaises dans les nappes penniques du Valais, *Eclogae Geologicae Helvetiae*, **99**, 363-407.

Sartori, M., Burri, M., Fierz-Dayer, E. and Curdy, P., 2007, Caractérisation pétrographique des éléments de construction de la nécropole du Petit-Chasseur et d'autres sites néolithiques de la région de Sion. *Bulletin d'études préhistoriques et archéologiques alpines (Aoste)*, **18,** 19-32.

Spear, F.S., 1989, Relative thermobarometry and metamorphic P-T paths. In: Daly J.S., Cliff R.A. and Yardley B.W.D. - *Evolution of Metamorphic Belts*, Geological Society, Oxford, 63-81.

Spear, F.S., Kohn, M.J., Florence, F.P. and Menard, T.,1991, A model for garnet and plagioclase growth in politic schist: implications for thermobarometry and P-T pat determinations. *Journal of metamorphic Geology*, **8**, 683-696.

Serra, M., Appolonia, L., Borghi, A., De Leo, S. and Rubinetto, V., 2012, A petrographic study of the anthropomorphic stelae from the megalithic area of Saint-Martin-de-Corléans (Aosta, Northern Italy). In: N. Meeks, C. Cartwright, A. Meek and A. Mongiatti (eds.), *Historical, Technology, Materials and Conservation. SEM and Microanalysis*. London, Archetype Publications, 196-198.



**Captions:**

Figure 1. Representative photographic documentation of the studied anthropomorphic stelae from the Megalithic Area of Saint-Martin-de-Corléans (Aosta, Northern Italy). A: example of ancient stelae (Stelae n. 13, foliated impure marble); B: example of evolved stelae (Stelae n. 30, massive marble with silicate layers).

Figure 2. Schematic geological map of the central sector of Aosta Valley (modified after Elter, 1987; Malusà, 2004; De Giusti *et al.*, 2004). Legend: A) Quaternary deposits; B) Austroalpine Domain: 1. Roisan zone, 2. Dent Blanche Nappe, 3. Mont Mary nappe, 4. Mont Emilius and Aguilles Rouge nappe; C) Gran Paradiso Nappe; D) *Fascio di Cogne*; E) Structurally composite

Piedmont Zone derived from the closure of the Mesozoic ocean: 1. Zermatt-Saas zone (nappe) consisting of eclogitic fragments of oceanic lithosphere, 2. Combin zone, including blueschist facies ophiolitic units and thin decollement cover units derived from debated continental basement, named Aouilletta in the study area west of Aosta; 3. Main bodies of metabasites in greenschists facies conditions (prasinites), amphibolites and minor eclogites; F) Middle Penninic Grand St. Bernard (Briançonnais) nappe system: 1. External Briançonnais nappe, 2. Internal Briançonnais nappe; G) Permian-Carboniferous Houillère Unit; H) Sion – Courmayeur zone;

Figure 3. Quantitative distribution, in percent occurrence, of identified lithologies among the analyzed stelae. In brackets, the ratio between the number of stelae formed by each lithotype and the total number of the studied stelae is given.

Figure 4. Representative microstructures of the investigated marbles, mineral abbreviation according to Kretz (1983). A: cross-polarized light image of foliated impure marble from the Aouilletta unit, external Combin zone. The foliation is defined by the iso-orientation of the phengitic mica (Stelae n. 38); B: light polarized image of calcschist from the Aouilletta unit, external Combin zone (Stelae n. 13). Pseudomorphs of white mica and calcite from lawsonite, preserving former graphite; C: backscattered SEM image of gray banded marble (Bardiglio) (Stelae n. 29), characterised by the iso-orientation of three varieties of di-octahedral mica: phengitic mica, margarite (not shown here) and paragonite. In the micaceous levels the phlogopite is interbedded; D: cross-polarized light image of massive marble with silicate layers showing albite poikiloblasts (Stelae n. 30). E: backscattered SEM image of massive marble with silicate layers marked by the occurrence of skeletal crystals of garnet grown around calcite and quartz (Stelae n. 6); F: light polarized image of prasinite from the Lower Piedmont Zone showing the typical greenschist facies metamorphic assemblage (Stelae n. 9); G: cross-polarized light image of milonitic orthogneiss from erratic blocks of glacial nature (Stelae n. 20); H: light polarized image of stilpnomelane-bearing quartzite of unknown provenance (Stelae n. 17).

Figure 5. A: Mesoscopic sample of the gray banded marble named “Bardiglio”, marked by layering defined by dark and light gray levels (Stelae n. 29). B: Detail relating to the silicate layers forming the Stelae n. 18. Notice the difference between the compact and isotropic lower portion of the stelae and the upper one of silicates shale (mod. after Appolonia *et al.*, 2010).

Figure 6. A, C, E: Si–$Al_{tot}$ classification diagram for di-octahedral micas respectively of foliated impure marble and calcschist (A) and of gray banded marble (Bardiglio marble) (C) of the Lower Piedmont Zone, and of massive marble with silicate layers of the Sion – Courmayeur Unit (E). The fields of high phengite (High-Phe), phengite (Phe) and muscovite (Ms) are reported according to Capedri *et al*. (2004). B, D, F: Chemical classification diagram for chlorites of foliated impure marble and calcschist (B) and of gray banded marble (Bardiglio marble) (D) of the Lower Piedmont Zone, and of massive marble with silicate layers of the Sion – Courmayeur Unit (E) (mod. after Hey, 1954).

**Tables:**

Table 1 - Mineralogical (major, minor and accessory minerals) comparison between the investigated stelae from the Megalithic Area of Saint-Martin-de-Corléans (Aosta, Northern Italy) and the reference quarry samples: A) Carbonate rocks; B) Silicate rocks. The thin sections named with brackets, (ABL001)-(ABL014), refer to thin section “similar” to the lithotypes used for the realization of the stelae.

Table 2 - Representative electron microprobe analyses of phengitic mica, calculated on the basis of 22 Ox.

Table 3 - Representative electron microprobe analyses of chlorite, calculated on the basis of 28 Ox.

Table 4 - Representative electron microprobe analyses of: phlogopite in the gray banded marble (stelae 29), calculated on the basis of 22 Ox; garnet (Stelae 6), calculated on the basis of 12 Ox, and amphibole (Stelae 40), calculated on the basis of 23 Ox, in the massive marble with silicate layers.

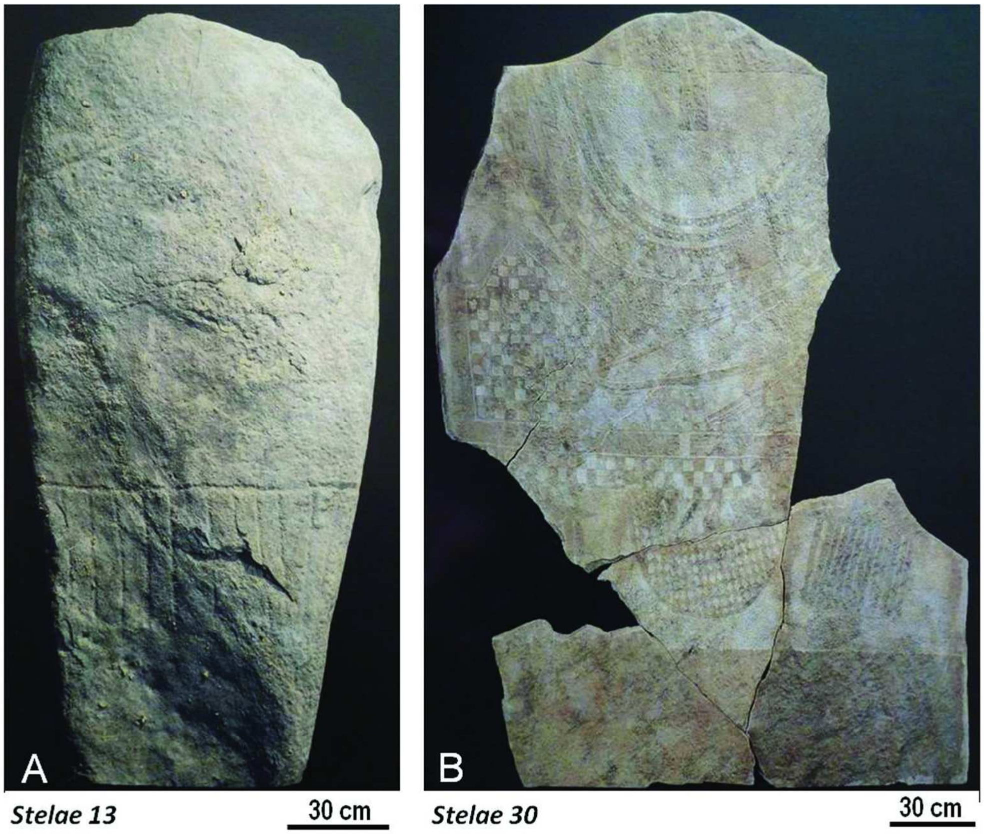


Figure 1. Representative photographic documentation of the studied anthropomorphic stelae from the Megalithic Area of Saint-Martin-de-Corléans (Aosta, Northern Italy). A: example of ancient stelae (Stelae n. 13, foliated impure marble); B: example of evolved stelae (Stelae n. 30, massive marble with silicate layers).
175x146mm (300 x 300 DPI)

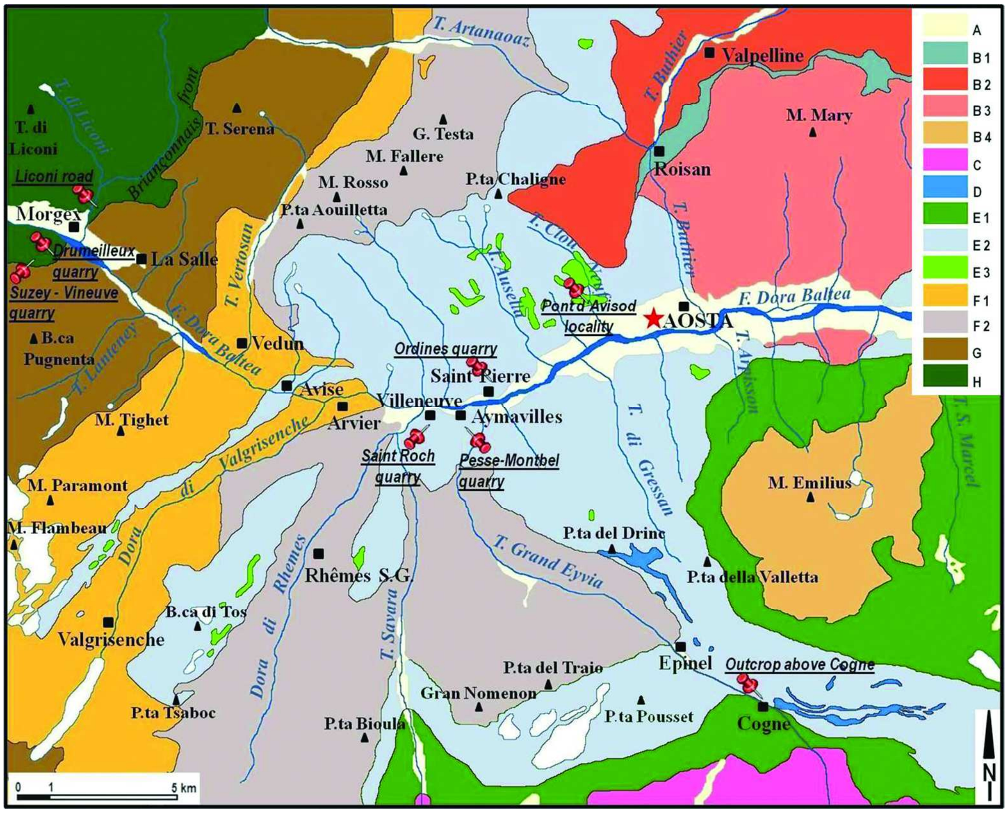


Figure 2. Schematic geological map of the central sector of Aosta Valley (modified after Elter, 1987; Malusà, 2004; De Giusti et al., 2004). Legend: A) Quaternary deposits; B) Austroalpine Domain: 1. Roisan zone, 2. Dent Blanche Nappe, 3. Mont Mary nappe, 4. Mont Emilius and Aguilles Rouge nappe; C) Gran Paradiso Nappe; D) Fascio di Cogne; E) Structurally composite Piedmont Zone derived from the closure of the Mesozoic ocean: 1. Zermatt-Saas zone (nappe) consisting of eclogitic fragments of oceanic lithosphere, 2. Combin zone, including blueschist facies ophiolitic units and thin decollement cover units derived from debated continental basement, named Aouilletta in the study area west of Aosta; 3. Main bodies of metabasites in greenschists facies conditions (prasinites), amphibolites and minor eclogites; F) Middle Penninic Grand St. Bernard (Briançonnais) nappe system: 1. External Briançonnais nappe, 2. Internal Briançonnais nappe; G) Permian-Carboniferous Houillère Unit; H) Sion – Courmayeur zone;
236x190mm (300 x 300 DPI)

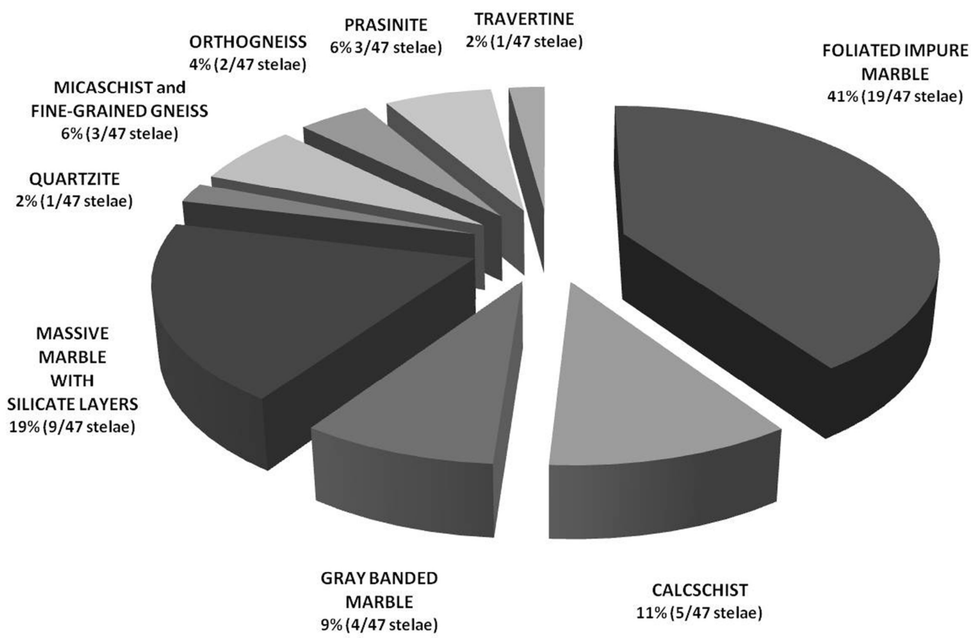


Figure 3. Quantitative distribution, in percent occurrence, of identified lithologies among the analyzed stelae. In brackets, the ratio between the number of stelae formed by each lithotype and the total number of the studied stelae is given.

200x134mm (300 x 300 DPI)

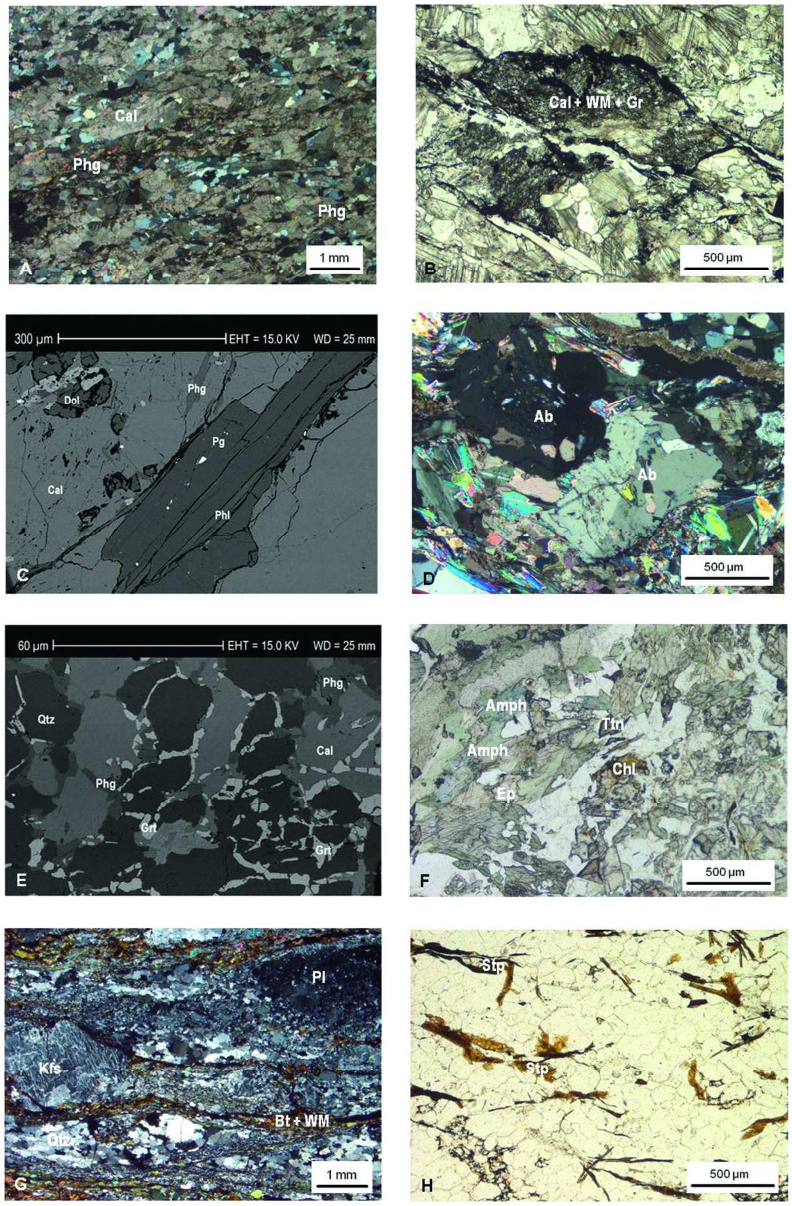


Figure 4. Representative microstructures of the investigated marbles, mineral abbreviation according to Kretz (1983). A: cross-polarized light image of foliated impure marble from the Aouilletta unit, external Combin zone. The foliation is defined by the iso-orientation of the phengitic mica (Stelae n. 38); B: light polarized image of calcschist from the Aouilletta unit, external Combin zone (Stelae n. 13). Pseudomorphs of white mica and calcite from lawsonite, preserving former graphite; C: backscattered SEM image of gray banded marble (Bardiglio) (Stelae n. 29), characterised by the iso-orientation of three varieties of di-octahedral mica: phengitic mica, margarite (not shown here) and paragonite. In the micaceous levels the phlogopite is interbedded; D: cross-polarized light image of massive marble with silicate layers showing albite poikiloblasts (Stelae n. 30). E: backscattered SEM image of massive marble with silicate layers marked by the occurrence of skeletal crystals of garnet grown around calcite and quartz (Stelae n. 6); F: light polarized image of prasinite from the Lower Piedmont Zone showing the typical greenschist facies metamorphic assemblage (Stelae n. 9); G: cross-polarized light image of milonitic orthogneiss from erratic blocks of glacial nature (Stelae n. 20); H: light polarized image of stilpnomelane-bearing quartzite of

unknown provenance (Stelae n. 17).
178x272mm (300 x 300 DPI)

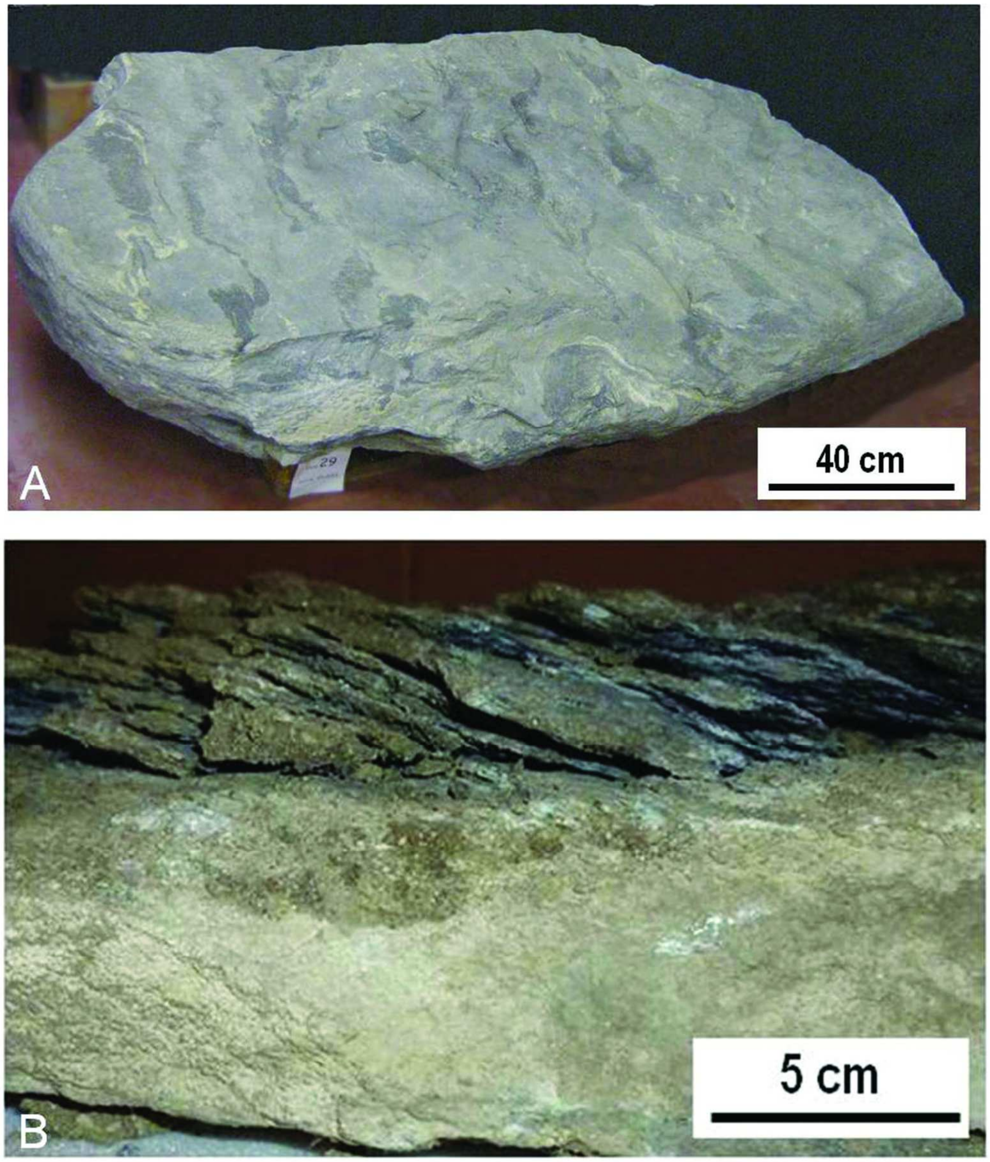


Figure 5. A: Mesoscopic sample of the gray banded marble named "Bardiglio", marked by layering defined by dark and light gray levels (Stelae n. 29). B: Detail relating to the silicate layers forming the Stelae n. 18. Notice the difference between the compact and isotropic lower portion of the stelae and the upper one of silicates shale (mod. after Appolonia et al., 2010).
152x177mm (300 x 300 DPI)

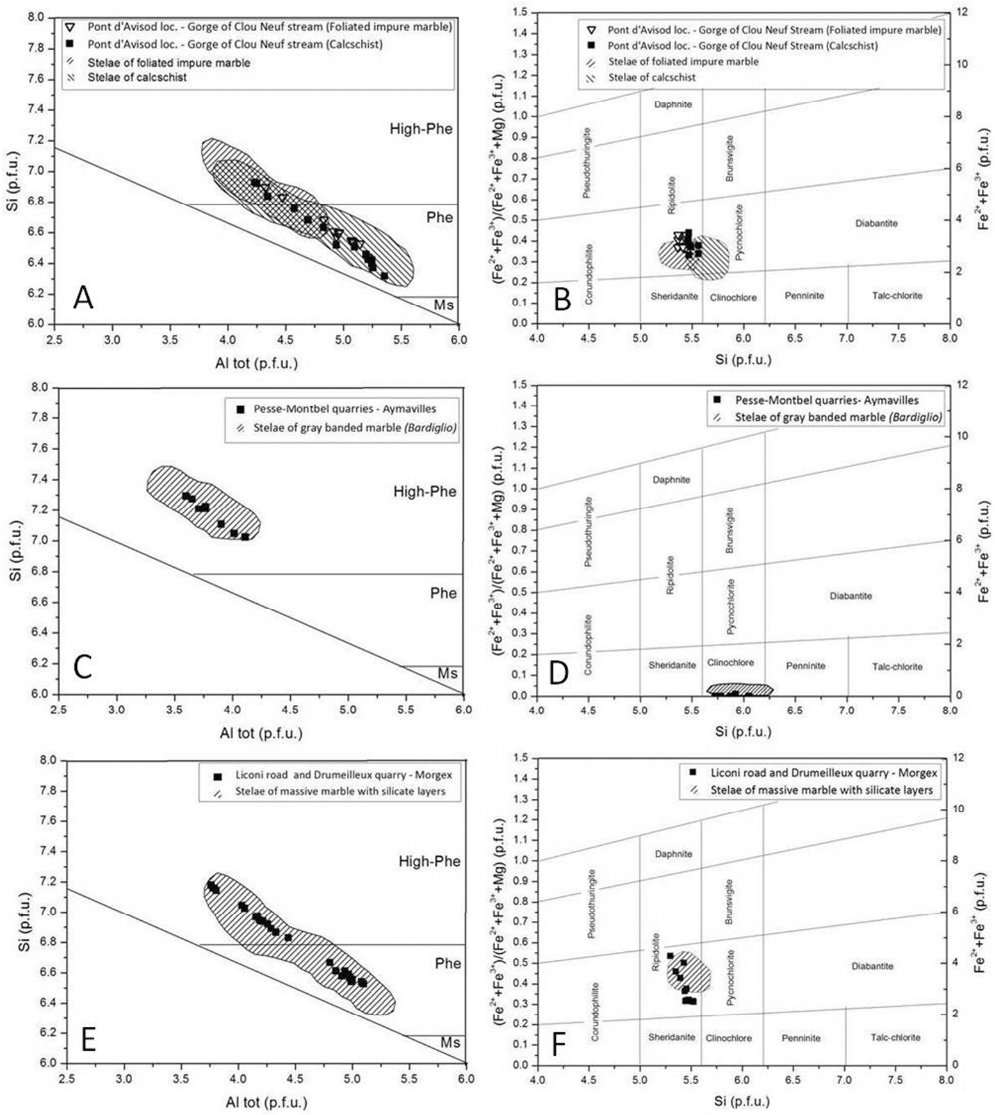


Figure 6. A, C, E: Si–Altot classification diagram for di-octahedral micas respectively of foliated impure marble and calcschist (A) and of gray banded marble (Bardiglio marble) (C) of the Lower Piedmont Zone, and of massive marble with silicate layers of the Sion – Courmayeur Unit (E). The fields of high phengite (High-Phe), phengite (Phe) and muscovite (Ms) are reported according to Capedri et al. (2004). B, D, F: Chemical classification diagram for chlorites of foliated impure marble and calcschist (B) and of gray banded marble (Bardiglio marble) (D) of the Lower Piedmont Zone, and of massive marble with silicate layers of the Sion – Courmayeur Unit (E) (mod. after Hey, 1954)

190x212mm (600 x 600 DPI)

| | STELAE/*QUARRY* | SAMPLE | MINERO - PETROGRAPHIC CHARACTERIZATION | *Calcite* | *Dolomite* | *Qtz* | *Ms* | *Pg* | *Phl* | *Bt* | *Chl* | *Ep* | *Ab* | *Lws* | *Cld* | *Amph* | *Rt* | *Ttn* | *Ap* | *Zrn* | *Tur* | *Grt* | *Gr* | *Fe sulphide* | *Fe oxide* |
|---|---|---|---|---|---|---|---|---|---|---|---|---|---|---|---|---|---|---|---|---|---|---|---|---|---|
| *FOLIATED IMPURE MARBLE* | St. 1 south | ABL032 | Impure foliated silicate marble | Main | Absent | xx | xx | | | | x | | xx | | | | | | | | x | | | | x |
| | St. 2 south | ABL033 | Impure foliated silicate marble | Main | Absent | xx | xx | | | | | | | | | | | | | | | | x | | x |
| | St. 4 | ABL035, C1 | Impure silicate marble | Main | Absent | xx | x | x | | | x | x | | ps | | | | x | x | | x | | x | x | x |
| | St. 6 south | (ABL007) | Impure silicate marble | Main | Absent | xx | xx | | | | xx | | x | ps | | | | | | | x | | x | | x |
| | St. 8 | ABL036 | Impure (weakly foliated) silicate marble | Main | Absent | xx | xx | | | | xx | | x | | | | | | | | x | | x | | x |
| | St. 12: T.I, roof. Cupping slabs | C5 | Impure foliated silicate marble | Main | Absent | xx | xx | | | | x | x | | ps | | | x | | x | | x | | x | x | x |
| | St. 13: T.I, NW pillar | C4 | Impure marble with pseudomorphs after Lws and micaceous levels | Main | Absent | xx | xx | | | | x | | x | ps | | | | | | | | | x | | x |
| | St. 16 | ABL038 | Impure foliated silicate marble | Main | Absent | xx | xx | | | | xx | | x | ps | | | | | | | x | | x | | x |
| | St. 23 | C8 | Silicate marble | Main | Absent | xx | xx | | | | x | x | | | | | | | x | | x | | x | | x |
| | St. 24 | ABL041 | Foliated marble with Ank | Main | Absent | xx | xx | | | | xx | x | xx | | | | | | | | x | | x | | x |
| | St. 27 | ABL044 | Impure foliated silicate marble | Main | Absent | xx | xx | x | | | xx | | | ps | | | x | | x | | x | | x | | x |
| | St. 28 | ABL045, ABL 045 bis | Impure foliated silicate marble | Main | Absent | xx | xx | | | | xx | | x | ps | | | | | | | x | | x | | x |
| | St. 32 | ABL047, ABL 047 bis | Very impure foliated silicate marble | Main | Absent | xx | xx | | | | x | x | | | | | | | | | x | | | | x |
| | St. 34 | C15 | Impure silicate marble | Main | Absent | xx | xx | x | | | x | x | xx | x, ps | | | x | | | x | x | | x | | x |
| | St. 35 | C16 | Impure foliated silicate marble | Main | Absent | xx | xx | | | | xx | x | | | | | x | | | | x | | x | | x |
| | St. 38 | ABL048 | Impure marble with WM | Main | Absent | xx | xx | | | | x | | x | | | | | | | | | | | | x |
| | St. 43 | ABL050 | Impure foliated silicate marble | Main | Absent | xx | xx | | | | x | x | xx | ps | | | | | | | x | | x | x | x |
| | St. XIV.9, Basement T.V | ABL062 | Impure silicate marble | Main | Absent | xx | xx | | | | x | x | | | | | | x | | | | | | | x |
| | T.II, hall - St. NW side | C12 | Impure marble with WM | Main | Absent | xx | xx | | | x | x | x | xx | | | | x | | x | x | x | | | | x |
| | *Pont d'Avisod loc.* | VR22 | Anisotrope impure foliated silicate marble | Main | Absent | xx | xx | x | | | xx | | xx | ps | | | | | | | x | | x | | x |
| | *Pont d'Avisod loc.* | ABL017 | Foliated silicate marble | Main | Absent | xx | xx | x | | | x | | x | | | | x | | x | | | | x | | x |
| *CALCSCHIST* | St. 21 | ABL040 | Calcschist with domains of Cal and WM | Main | Absent | xx | xx | | | | | x | | | | | | x | | | x | | x | | x |
| | St. 22 | C7 | Calcschist with domains of Cal and WM | Main | Absent | xx | xx | x | | | xx | x | x | | | | x | x | x | | x | | x | | x |
| | St. 26 | ABL043 | Calcschist with Ank | Main | Absent | xx | xx | x | | | xx | | xx | | | | | x | x | x | x | | | | x |
| | St. 36 | ABL067 | Calcschist with Ank | Main | Absent | xx | xx | | | | xx | x | x | | | | x | | | | x | | x | | x |
| | T.VII, SW pillar | ABL028 | Calcschist with Ank | Main | Absent | xx | xx | | | | xx | x | xx | | | | | | | | x | | | | x |
| | *Pont d'Avisod loc.* | ABL015, VR23 | Calcschist with pseudomorphs after Lws and transposed stable Cld, with WM in two phases of sin-metamorphic deformation | Main | Absent | xx | xx | x | | | x | | xx | x, ps | x | | | | | | x | | | x | x |
| | *Pont d'Avisod loc.* | ABL016 | Calcschist with late growth of Ab and Bt | Main | Absent | xx | xx | x | | x | | | xx | | | | | | | | | | | | x |
| | *Outcrop above Cogne* | CS16 | Calcschist | Main | x | xx | xx | | | | | | x | | | | | | | | x | | | x | x |
| *GRAY BANDED MARBLE* | St. 3 south | ABL034 | Impure silicate marble with dolomitic layers | Main | Main | xx | xx | x | x | | | | x | | | | | | x | | | | | x | x |
| | St. 29 | C13 | Weakly impure silicate marble with dolomitic layers | Main | Main | x | x | x | x | | x | | x | | | | x | x | x | | | | | x | x |
| | St. 31 | ABL 046, ABL 046 bis | Weakly impure silicate marble with dolomitic layers | Main | Main | x | x | | | | | x | x | | | | | | | | | | | | x |
| | T.II, NE pillar | C10 | Weakly impure silicate marble with dolomitic layers and variuos micaceous compositional varieties | Main | Main | x | x | | | | | | x | | | | | | | | | | x | | x |
| | *Saint Roch quarry - Villeneuve* | ABL021, VR8, VR7 | Impure marble "Bardiglio of Villeneuve" | Main | Main | xx | xx | x | | | | | x | ps | | | | | | | | | | x | x |
| | *Saint Roch quarry - Villeneuve* | ABL022 | Impure marble "Bardiglio of Villeneuve" | Main | Main | xx | xx | x | | | | | | x | | | | | | | | | | | x |
| | *Saint Roch quarry - Villeneuve* | ABL023 | Very pure marble "Bardiglio of Villeneuve" | Main | Absent | x | x | x | | | | | | | | | | | | | | | | | x |
| | *Saint Roch quarry - Villeneuve* | VR9 | Very impure marble "Bardiglio of Villeneuve" | Main | Main | xx | xx | x | | | x | | | ps | | | | | x | | | | x | x | x |
| | *Saint Roch quarry - Villeneuve* | VR10 | Very impure marble "Bardiglio of Villeneuve" | Main | Absent | xx | xx | x | | | x | | xx | ps | | | | | | | x | | x | x | x |
| | *Pesse-Montbel quarry - Aymavilles* | ABL024, ABL025 | Calcitic and dolomitic impure marble | Main | Main | x | x | x | x | | x | | x | | | | | | | | | | | x | x |

| | | | | | | | | | | | | | | | | | | | | | | | |
|---|---|---|---|---|---|---|---|---|---|---|---|---|---|---|---|---|---|---|---|---|---|---|---|
| | *Ordines quarry - Saint Pierre* | ABL059, VR14, VR15 | Impure marble | Main | Main | xx | xx | x | | x | | xx | ps | | x | x | | x | | | x | x | x |
| | *Ordines quarry - Saint Pierre* | ABL061, VR11, VR12, VR13 | Impure (weakly foliated) silicate marble | Main | Absent | xx | xx | x | | | | | ps | | | | | | | | x | | x |
| | *Ordines quarry - Saint Pierre* | VR16 | Calcschist | Main | Absent | xx | xx | x | | x | | x | ps | | | | | | x | | x | | x |
| *MASSIVE MARBLE WITH SILICATE LAYERS* | St. 4 south | C17 | Weakly anisotrope marble with centimetric silicate layers | Main | Absent | xx | x | | | x | x | xx | | | x | | x | | | | | | x |
| | | ABL068 | Calcite-bearing micaschist | x | Absent | Main | xx | | | x | | xx | | | | x | | | | | x | | x |
| | St. 5 | C2 | Calcschist | Main | Absent | Main | x | | | x | x | xx | | | | | | | | | x | x | x |
| | | C2a | Quartzitic - albitic impure marble | Main | Absent | xx | xx | | | | | xx | | | | | | | | | x | x | x |
| | St. 6 | C3 | Impure marble with Grt | Main | Absent | xx | xx | | | x | x | xx | | | | x | x | x | | x | | | x |
| | St. 18 | ABL039a | Micaschist | Absent | Absent | Main | Main | | | x | x | xx | | | | | | x | x | | x | | x |
| | | ABL039b | Impure silicate marble | Main | Absent | xx | x | | | x | x | xx | | | | x | | x | x | | x | | x |
| | St. 25 | ABL042 | Impure silicate marble | Main | Absent | xx | x | | | x | | xx | | | | | | | x | | | x | x |
| | St. 30 | ABL065 | Marble with centimetric silicate layers | Main | Absent | xx | xx | x | | xx | x | xx | ps | | | x | x | | x | | x | | x |
| | | ABL049 | Impure marble with silicate layers | Main | Absent | xx | xx | | x | x | x | x | ps | | | x | | | x | | x | x | x |
| | St. 40 | C14 | Micaceous and amphibolitic portion of marble with silicate layers | Absent | Absent | xx | xx | | xx | xx | xx | xx | | x | | x | | | | | | | x |
| | T.II, roof | C9 | Micaceous portion of marble with silicate layers | Absent | Absent | xx | Main | | x | x | xx | x | | | | x | | | x | | | | x |
| | Interface St. 4 south and St. 6 south | (ABL002) | Impure marble with silicate layers | Main | Absent | xx | xx | | | x | x | xx | ps | | | x | | | x | | x | x | x |
| | *Liconi road - Morgex* | ABL018, ABL019 | Marble with domains of WM, alternated with domains of Qtz and carbonates | Main | Absent | x | x | x | | x | | x | | | | x | | | | | | x | x |
| | *Liconi road - Morgex* | VR1, VR2 | Weakly impure silicate marble | Main | Absent | xx | x | x | | x | x | x | | | | | | | x | | x | | |
| | *Liconi road - Morgex* | VR3 | Impure foliated silicate marble | Main | Absent | xx | xx | x | | x | x | xx | ps | | | x | | x | x | | x | x | x |
| | *Suzey-Vineuve quarry - Morgex* | ABL020 | Impure silicate marble | Main | Absent | xx | xx | | | x | x | x | ps | | | x | x | | | | | x | x |
| | *Drumeilleux quarry - Morgex* | VR4 | Impure silicate marble | Main | Absent | xx | x | x | | x | | xx | | | x | | x | | x | | | x | x |
| *TRAV.* | T. V, NW pillar | ABL029 | Travertine with silicate inclusions | Main | Absent | x | x | | | | x | x | | | | | | | | | | | |

St., Stelae; T., Tomb; NW, North-West; SW, South-West; NE, North-East; xx = <10% vol.; x = accessory mineral.
Qtz, Quartz; Ms, Muscovite; Pg, Paragonite; Phl, Phlogopite; Bt, Biotite; Chl, Chlorite; Ep, Epidote; Ab, Albite; Lws, Lawsonite; Cld, Chloritoid; Amph, Amphibole; Rt, Rutile; Ttn, Titanite; Ap, Apatite; Zrn, Zircon; Tur, Tourmaline; Grt, Garnet; Gr, Graphite.

| | | | | | | | | |
|---|---|---|---|---|---|---|---|---|
| QUARTZITE | St. 17 | ABL064 | Quartzite with Stp | Main | Absent | x | x | |
| MICASCHIST and FINE-GRAINED GNEISS | passage between T.V | ABL027 | Garnet-mica schist | Main | Main | xx | xx | |
| | T.II, SW upright | C11 | gneiss from albitic | Main | Main | x | x | |
| | T.VII, NE upright | ABL031 | gneiss from low-grade | Main | Main | x | x | |
| ORTHOGNEISS | St. 11 = T.I, SE upright | ABL037 | Milonitic orthogneiss | Main | Main | x | x | |
| | St. 20 | C6 | Orthogneiss with milonitic domains | Main | Main | xx | xx | |
| PRASINITE | St. 9 | ABL 063 | Prasinite | Main | Absent | xx | xx | |
| | St. A, T.II SE | ABL026 | Prasinitic gneiss | Main | Absent | x | x | |
| | St. "P" | ABL066 | Prasinitic gneiss | Main | Main | x | xx | |
| TRAVERTINE | T.V, NW upright | ABL029 | Travertine with silicate inclusions | Main | Main | x | xx | |
| | | | | Main | Main | 30% | xx | |
| | - | | | Main | Absent | xx | xx | |
| | | | | Main | Main | x | x | |
| | | | | Main | Main | x | x | |
| | | | | Main | Main | xx | xx | |
| | | | | Main | Absent | xx | x | |
| | | | | Main | Absent | xx | 25% | |
| | | | | Main | Absent | xx | xx | |
| | | | | Main | Absent | x | xx | |
| | | | | Main | Absent | xx | xx | |
| | | | | Main | Main | xx | xx | |
| | | | | Main | Main | xx | xx | |
| | | | | Main | Absent | 35% | xx | |
| | | | | Main | Absent | xx | x | |
| | | | | Main | Absent | 60% | xx | |
| | | | | Main | Absent | 40% | x | |
| | | | | Main | Absent | xx | xx | |
| | | | | Main | Absent | xx | xx | |
| | | | | Main (below) | | | | |
| | | | | Absent (over) | Absent | 5% (inf); 45% (su\|x (inf); 50% (sup) | | |
| | | | | Main | Absent | 30% | x | |
| | | | | Main | Absent | 35% | xx | |
| | | | | Main | Absent | xx | xx | |
| | | | | Main | Absent | 30% | xx | |
| | | | | Absent | Absent | 25% | 35% con Bt e Chl | 35 |
| | | | | | | xx | 70% | |

| | | | |
|---|---|---|---|
| Main | Absent | 30% | xx |
| Main | Absent | x | x |
| Main | Absent | x | x |
| Main | Absent | xx | x |
| Main | Absent | x | x |
| Main | Absent | xx | xx |
| Main | Absent | xx | xx |
| Main | Absent | xx | x |
| Main | Absent | x | 45% |
| Main | Absent | x | x |

| | | | | | | | | | |
|---|---|---|---|---|---|---|---|---|---|
| | | | x | | | | | | |
| | | | x (Ab) | | | | x | | |
| | x | | x (Ab) | | x | x | x | | |
| | | x (Ep) | x (Ab) | | | | | | |
| | | | x (Ab) | | | | | | |
| | | | x (Ab) | pseud. | | | | | |
| | | | | x | | | | | |
| | | | x (Ab) | | | | | | |
| | x | | x (Ab) | pseud. | | | | | |
| | x | | | pseud. | | | x | | |
| | x | | xx (Ab) | pseud. | | | | | x |
| | x | | | | | | | | |
| | x | | x (Ab) | | | | | | |
| | | | xx (Ab) | pseud. | x | x | | x | |
| | x | | xx (Ab) | pseud. | | | | | |
| | | | | pseud. | | | | | |
| | | | | pseud. | | | | | |
| | | | | pseud. | | | | | |
| | | | | pseud. | | | | | |
| | | | xx (Ab) | pseud. | | x | | | |
| | x | | x (Ab) | pseud. | x | | x | x | |
| | x | | x (Ab) | pseud. | | | | | x |
| | x | x (Ep, Aln) | xx (Ab) | | x | | x | | |
| | x | | xx (Ab) | | | x | | | |
| | x | x (Ep) | xx (Ab) | | | | | | |
| | | | xx (Ab) | | | | | | |
| | x | x (Ep) | xx (Ab) | | | x | x | x | |
| | x | x (Ep (inf)) | xx (Ab) | | | x (inf) | | x | x |
| | x | | xx (Ab) | | | | | | x |
| | xx | x (Ep, Aln) | xx (Ab) | pseud. | | x | x | | x |
| | x | x (Ep, Zo) | xx (Ab) | pseud. (ABL010) | | x | | | x |
| x | x | x (Ep, Zo) | x (Ab) | pseud. | | x | | | x |
| % con Wmca e C | 5% con Bt e Wmc | xx (Ep, Zo, Aln) | 30% (Ab) | | | x | | | |
| x | x | xx (Czo) | x ( Ab) | | | x | | | x |

| | | | | | | | | |
|---|---|---|---|---|---|---|---|---|
| x | x (Zo) | xx (Ab) | pseud. | | x | | | x |
| x | | x (Ab) | | | x | | | |
| | | x (Ab) | | | | | | |
| x | x (Czo) | x (Ab) | | | | | | |
| x | x (Czo) | x (Ab) | | | | | | x |
| x | x (Ep) | xx (Ab) | pseud. | | x | | x | x |
| | | x (Ab) | pseud. | | x | | x | |
| x | | xx (Ab) | | x | | x | | x |
| x | x (Ep) | x | pseud. | | | | | x |
| | x (Ep) | x (Ab) | | | | | | |

| | | | |
|---|---|---|---|
| | | | x |
| | | x | x |
| | | x | x |
| | | | x |
| | x | | x |
| | | | x |
| | | | x |
| | | | x |
| | | x | x |
| | | | x |
| | x | x | x |
| | x | x | x |
| | | x | x |
| | | | x |
| | | x | x |
| | | | x |
| | x | | x |
| | x | | x |
| | x | | x |
| | x | | x |
| | x | x | x |
| | | x | |
| | x | | x |
| | | | x |
| | x | | x |
| | x | x | x |
| | x | x | x |
| x | | | x |
| | x | | x |
| | | x | x |
| | x | | x |
| | x | x | x |
| | x | x | x |
| | | | x |
| | | | x |

| | | | |
|---|---|---|---|
| | x | x | x |
| | | x | x |
| | | | x |
| | x | | |
| | x | | |
| | x | x | x |
| | | | x |
| | | x | x |
| | x | x | x |

| | STELAE | SAMPLE | MINERO - PETROGRAPHIC CHARACTERIZATION | *Qtz* | *WM* | *Bt* | *Chl* | *Ep* | *Fsp* | *Amph* | *Rt* | *Ttn* | *Zrn* | *Tur* | *Grt* | *Stp* | *Fe sulphide* | *Fe oxide* |
|---|---|---|---|---|---|---|---|---|---|---|---|---|---|---|---|---|---|---|
| *QUARTZITE* | St. 17 | ABL064 | Quartzite with Stp | 75% | x | | x | | x (Ab) | | | | | x | | 20% | | x |
| *MICASCHIST and FINE-GRAINED GNEISS* | Great slab in passage between T. V and T. VII | ABL027 | Garnet mica-schist | 35% | 40% | | x | x | 20% (Ab) | | | | | | x | | | |
| | T. II, SW pillar | C11 | Fine-grained gneiss from albitic micaschist | 40% | 20-30% | x (in reaction with chl) | x (in reaction with bt) | | 20-30% (Ab) | | | | x | | | | | x |
| | T. VII, NE pillar | ABL031 | Fine-grained gneiss from low-grade micaschist | 30% | 40% | | x | | 25-30% (Ab) | | | | | | | | | x |
| *ORTHOGNEISS* | St. 11 = T. I, SE pillar | ABL037 | Milonitic orthogneiss | 40% | x | xx | | x | x (Ab); 40% (K-Fsp) | | | | | | x | | | x |
| | St. 20 | C6 | Orthogneiss with milonitic domains | 70% | xx | x | x | x | xx (Ab); xx (K-Fsp) | | | x | x | | x | | | x |
| *PRASINITE* | St. 9 | ABL 063 | Prasinite | x | | | xx | 35% | x (Ab) | 50% | x | x | | | | | | x |
| | St. A, T. II SE | ABL026 | Prasinitic gneiss | xx | xx | xx | | xx | 30% (Ab) | xx | | x | | | x | | | x |
| | St. "P" | ABL066 | Prasinitic gneiss | xx | x | xx | | xx | xx (Ab) | xx | | x | | | x | | | x |

St., Stelae; T., Tomb; SW, South-West; NE, North-East; SE, South-East; % = main phase; xx = <10% vol.; x = accessory mineral.
Qtz, Quartz; WM, White mica; Bt, Biotite; Chl, Chlorite; Ep, Epidote; Fsp, Feldspar; Amph, Amphibole; Rt, Rutile; Ttn, Titanite; Zrn, Zircon; Tur, Tourmaline; Grt, Garnet; Stp, Stilpnomelane.

| | | | | | | | | |
|---|---|---|---|---|---|---|---|---|
| QUARTZITE | **St. 17** | ABL064 | Quartzite with Stp | Main | Absent | x | x | |
| MICASCHIST and FINE-GRAINED GNEISS | **passage between T.V** | ABL027 | Garnet-mica schist | Main | Main | xx | xx | |
| | **T.II, SW upright** | C11 | gneiss from albitic | Main | Main | x | x | |
| | **T.VII, NE upright** | ABL031 | gneiss from low-grade | Main | Main | x | x | |
| ORTHOGNEISS | **St. 11 = T.I, SE upright** | ABL037 | Milonitic orthogneiss | Main | Main | x | x | |
| | **St. 20** | C6 | Orthogneiss with milonitic domains | Main | Main | xx | xx | |
| PRASINITE | **St. 9** | ABL 063 | Prasinite | Main | Absent | xx | xx | |
| | **St. A, T.II SE** | ABL026 | Prasinitic gneiss | Main | Absent | x | x | |
| | **St. "P"** | ABL066 | Prasinitic gneiss | Main | Main | x | xx | |
| TRAVERTINE | **T.V, NW upright** | ABL029 | Travertine with silicate inclusions | Main | Main | x | xx | |
| | | | | Main | Main | 30% | xx | |
| | - | | | Main | Absent | xx | xx | |
| | | | | Main | Main | x | x | |
| | | | | Main | Main | x | x | |
| | | | | Main | Main | xx | xx | |
| | | | | Main | Absent | xx | x | |
| | | | | Main | Absent | xx | 25% | |
| | | | | Main | Absent | xx | xx | |
| | | | | Main | Absent | x | xx | |
| | | | | Main | Absent | xx | xx | |
| | | | | Main | Main | xx | xx | |
| | | | | Main | Main | xx | xx | |
| | | | | Main | Absent | 35% | xx | |
| | | | | Main | Absent | xx | x | |
| | | | | Main | Absent | 60% | xx | |
| | | | | Main | Absent | 40% | x | |
| | | | | Main | Absent | xx | xx | |
| | | | | Main | Absent | xx | xx | |
| | | | | Main (below) | | | | |
| | | | | Absent (over) | Absent | 5% (inf); 45% (su\|x (inf); 50% (sup) | | |
| | | | | Main | Absent | 30% | x | |
| | | | | Main | Absent | 35% | xx | |
| | | | | Main | Absent | xx | xx | |
| | | | | Main | Absent | 30% | xx | |
| | | | | Absent | Absent | 25% | 35% con Bt e Chl | 35 |
| | | | | | | xx | 70% | |

| | | | |
|---|---|---|---|
| Main | Absent | 30% | xx |
| Main | Absent | x | x |
| Main | Absent | x | x |
| Main | Absent | xx | x |
| Main | Absent | x | x |
| Main | Absent | xx | xx |
| Main | Absent | xx | xx |
| Main | Absent | xx | x |
| Main | Absent | x | 45% |
| Main | Absent | x | x |

| | | | | | | | | | |
|---|---|---|---|---|---|---|---|---|---|
| | | | x | | | | | | |
| | | | x (Ab) | | | | x | | |
| | x | | x (Ab) | | x | x | x | | |
| | | x (Ep) | x (Ab) | | | | | | |
| | | | x (Ab) | | | | | | |
| | | | x (Ab) | pseud. | | | | | |
| | | | | x | | | | | |
| | | | x (Ab) | | | | | | |
| | x | | x (Ab) | pseud. | | | | | |
| | x | | | pseud. | | | x | | |
| | x | | xx (Ab) | pseud. | | | | | x |
| | x | | | | | | | | |
| | x | | x (Ab) | | | | | | |
| | | | xx (Ab) | pseud. | x | x | | x | |
| | x | | xx (Ab) | pseud. | | | | | |
| | | | | pseud. | | | | | |
| | | | | pseud. | | | | | |
| | | | | pseud. | | | | | |
| | | | | pseud. | | | | | |
| | | | xx (Ab) | pseud. | | x | | | |
| | x | | x (Ab) | pseud. | x | | x | x | |
| | x | | x (Ab) | pseud. | | | | | x |
| | x | x (Ep, Aln) | xx (Ab) | | x | | x | | |
| | x | | xx (Ab) | | | x | | | |
| | x | x (Ep) | xx (Ab) | | | | | | |
| | | | xx (Ab) | | | | | | |
| | x | x (Ep) | xx (Ab) | | | x | x | x | |
| | x | x (Ep (inf)) | xx (Ab) | | | x (inf) | | x | x |
| | x | | xx (Ab) | | | | | | x |
| | xx | x (Ep, Aln) | xx (Ab) | pseud. | | x | x | | x |
| | x | x (Ep, Zo) | xx (Ab) | pseud. (ABL010) | | x | | | x |
| x | x | x (Ep, Zo) | x (Ab) | pseud. | | x | | | x |
| % con Wmca e | 5% con Bt e Wm | xx (Ep, Zo, Aln) | 30% (Ab) | | | x | | | |
| x | x | xx (Czo) | x ( Ab) | | | x | | | x |

| | | | | | | | | |
|---|---|---|---|---|---|---|---|---|
| x | x (Zo) | xx (Ab) | pseud. | | x | | | x |
| x | | x (Ab) | | | x | | | |
| | | x (Ab) | | | | | | |
| x | x (Czo) | x (Ab) | | | | | | |
| x | x (Czo) | x (Ab) | | | | | | x |
| x | x (Ep) | xx (Ab) | pseud. | | x | | x | x |
| | | x (Ab) | pseud. | | x | | x | |
| x | | xx (Ab) | | x | | x | | x |
| x | x (Ep) | x | pseud. | | | | | x |
| | x (Ep) | x (Ab) | | | | | | |

| | | | |
|---|---|---|---|
| | | | x |
| | | x | x |
| | | x | x |
| | | | x |
| | x | | x |
| | | | x |
| | | | x |
| | | | x |
| | | x | x |
| | | | x |
| | x | x | x |
| | x | x | x |
| | | x | x |
| | | | x |
| | | x | x |
| | | | x |
| | x | | x |
| | x | | x |
| | x | | x |
| | x | | x |
| | x | x | x |
| | | x | |
| | x | | x |
| | | | x |
| | x | | x |
| | x | x | x |
| | x | x | x |
| x | | | x |
| | x | | x |
| | | x | x |
| | x | | x |
| | x | x | x |
| | x | x | x |
| | | | x |
| | | | x |

| | | | |
|---|---|---|---|
| | x | x | x |
| | | x | x |
| | | | x |
| | x | | |
| | x | | |
| | x | x | x |
| | | | x |
| | | x | x |
| | x | x | x |

| | Foliated impure marble and calcschist | | | | | | Gray banded marble | | | | Massive marble with silicate layers | | | |
|---|---|---|---|---|---|---|---|---|---|---|---|---|---|---|
| | Stelae 27 - Stelae 26 | | | Pont d'Avisod Quarry | | | Stelae 29 | | Aymavilles quarry | | Stelae 30 | | Licony road | |
| ANAL. NR. | Ph 1 | Ph 2 | Ph 3 | Ph 4 | Ph 5 | Ph 6 | Ph 7 | Ph 8 | Ph 9 | Ph 10 | Ph 11 | Ph 12 | Ph 13 | Ph 14 |
| $SiO_2$ | 49.34 | 49.36 | 53.21 | 49.72 | 50.46 | 50.30 | 56.16 | 57.10 | 55.95 | 55.95 | 49.85 | 49.41 | 52.83 | 52.98 |
| $TiO_2$ | bdl | bdl | bdl | bdl | bdl | bdl | bdl | bdl | bdl | bdl | 0.48 | bdl | bdl | bdl |
| $Al_2O_3$ | 35.29 | 36.22 | 27.37 | 32.69 | 32.18 | 31.75 | 23.28 | 21.98 | 23.82 | 23.42 | 33.42 | 33.12 | 27.23 | 27.11 |
| FeO | 0.58 | 0.77 | 1.81 | 1.42 | 1.56 | 1.53 | bdl | bdl | bdl | bdl | 1.59 | 1.62 | 2.47 | 2.59 |
| MnO | bdl | bdl | bdl | bdl | bdl | bdl | bdl | bdl | bdl | bdl | bdl | bdl | bdl | bdl |
| MgO | 1.06 | 0.75 | 3.67 | 1.56 | 1.61 | 1.85 | 6.23 | 6.73 | 5.98 | 6.16 | 1.54 | 1.60 | 3.35 | 3.36 |
| CaO | bdl | bdl | bdl | bdl | bdl | bdl | bdl | bdl | bdl | bdl | bdl | bdl | bdl | bdl |
| $Na_2O$ | 0.70 | 0.86 | bdl | 0.64 | 0.52 | 0.56 | bdl | bdl | bdl | bdl | 0.58 | 0.58 | 0.34 | 0.34 |
| $K_2O$ | 9.69 | 9.12 | 10.74 | 9.12 | 9.90 | 9.70 | 9.39 | 10.05 | 9.88 | 9.83 | 9.95 | 9.83 | 9.91 | 10.10 |
| ***** | ***** | ***** | ***** | ***** | ***** | ***** | ***** | ***** | ***** | ***** | ***** | ***** | ***** | ***** |
| Total | 96.66 | 97.08 | 96.82 | 95.14 | 96.22 | 95.69 | 95.07 | 95.85 | 95.64 | 95.35 | 97.42 | 96.15 | 96.14 | 96.48 |
| | | | | | | | | | | | | | | |
| Si | 6.386 | 6.346 | 6.942 | 6.544 | 6.594 | 6.606 | 7.322 | 7.412 | 7.274 | 7.294 | 6.450 | 6.474 | 6.938 | 6.946 |
| Al IV | 1.616 | 1.656 | 1.060 | 1.458 | 1.406 | 1.394 | 0.680 | 0.590 | 0.726 | 0.706 | 1.552 | 1.528 | 1.062 | 1.056 |
| | | | | | | | | | | | | | | |
| Al VI | 3.770 | 3.832 | 3.150 | 3.614 | 3.552 | 3.522 | 2.898 | 2.774 | 2.924 | 2.892 | 3.546 | 3.586 | 3.154 | 3.134 |
| Ti | - | - | - | - | - | - | - | - | - | - | 0.048 | - | - | - |
| Fe | 0.064 | 0.084 | 0.198 | 0.156 | 0.170 | 0.168 | - | - | - | - | 0.172 | 0.178 | 0.272 | 0.284 |
| Mn | - | - | - | - | - | - | - | - | - | - | - | - | - | - |
| Mg | 0.206 | 0.144 | 0.714 | 0.306 | 0.314 | 0.362 | 1.212 | 1.302 | 1.158 | 1.198 | 0.298 | 0.312 | 0.656 | 0.656 |
| | | | | | | | | | | | | | | |
| Ca | - | - | - | - | - | - | - | - | - | - | - | - | - | - |
| Na | 0.176 | 0.214 | - | 0.162 | 0.132 | 0.144 | - | - | - | - | 0.146 | 0.148 | 0.088 | 0.086 |
| K | 1.600 | 1.496 | 1.788 | 1.532 | 1.652 | 1.626 | 1.562 | 1.664 | 1.640 | 1.636 | 1.642 | 1.642 | 1.662 | 1.690 |
| | | | | | | | | | | | | | | |
| Z | 8.000 | 8.000 | 8.000 | 8.000 | 8.000 | 8.000 | 8.000 | 8.000 | 8.000 | 8.000 | 8.000 | 8.000 | 8.000 | 8.000 |
| Y | 4.036 | 4.058 | 4.062 | 4.076 | 4.036 | 4.052 | 4.110 | 4.076 | 4.082 | 4.090 | 4.062 | 4.076 | 4.080 | 4.074 |
| X | 1.774 | 1.710 | 1.788 | 1.694 | 1.784 | 1.770 | 1.562 | 1.664 | 1.640 | 1.636 | 1.788 | 1.790 | 1.748 | 1.776 |

| | Foliated impure marble and calcschist | | | | | | Gray banded marble | | | | Massive marble with silicate layers | | | |
|---|---|---|---|---|---|---|---|---|---|---|---|---|---|---|
| | Stelae 27 - Stelae 26 | | | Pont d'Avisod Quarry | | | Stelae 29 | | Aymavilles quarry | | Stelae 30 | | Licony road | |
| ANAL. NR. | Chl 1 | Chl 2 | Chl 3 | Chl 4 | Chl 5 | Chl 6 | Chl 7 | Chl 8 | Chl 9 | Chl 10 | Chl 11 | Chl 12 | Chl 13 | Chl 14 |
| $SiO_2$ | 27.08 | 27.31 | 28.62 | 26.91 | 27.37 | 27.38 | 31.64 | 31.03 | 30.37 | 32.02 | 26.36 | 26.83 | 27.84 | 25.94 |
| $Al_2O_3$ | 23.89 | 24.05 | 21.27 | 22.91 | 22.35 | 22.92 | 22.34 | 21.85 | 22.58 | 21.71 | 22.32 | 22.86 | 22.78 | 21.95 |
| FeO | 18.96 | 17.60 | 18.74 | 20.70 | 17.58 | 19.54 | 0.81 | 1.06 | bdl | 0.57 | 22.50 | 22.06 | 17.49 | 25.89 |
| MgO | 18.66 | 19.12 | 20.68 | 17.71 | 19.28 | 18.78 | 33.45 | 32.56 | 32.14 | 32.54 | 17.10 | 17.40 | 21.18 | 14.39 |
| CaO | bdl | bdl | bdl | bdl | bdl | bdl | 0.30 | bdl | bdl | bdl | bdl | bdl | bdl | bdl |
| ***** | ****** | ****** | ***** | ***** | ***** | ***** | ***** | ***** | ***** | ***** | ***** | ***** | ***** | ***** |
| Total | 88.59 | 88.08 | 89.32 | 88.23 | 86.58 | 88.62 | 88.54 | 86.50 | 85.09 | 86.84 | 88.30 | 89.14 | 89.29 | 88.17 |
| | | | | | | | | | | | | | | |
| Si | 5.414 | 5.449 | 5.670 | 5.458 | 5.565 | 5.490 | 5.766 | 5.787 | 5.724 | 5.922 | 5.408 | 5.424 | 5.484 | 5.430 |
| Al IV | 2.586 | 2.551 | 2.330 | 2.542 | 2.435 | 2.510 | 2.234 | 2.213 | 2.276 | 2.078 | 2.592 | 2.576 | 2.516 | 2.570 |
| | | | | | | | | | | | | | | |
| Al VI | 3.043 | 3.102 | 2.637 | 2.936 | 2.921 | 2.909 | 2.564 | 2.591 | 2.738 | 2.654 | 2.805 | 2.875 | 2.773 | 2.843 |
| Fe | 3.170 | 2.936 | 3.104 | 3.512 | 2.990 | 3.277 | 0.124 | 0.166 | - | 0.088 | 3.860 | 3.730 | 2.881 | 4.530 |
| Mg | 5.558 | 5.687 | 6.106 | 5.354 | 5.846 | 5.614 | 9.089 | 9.054 | 9.031 | 8.971 | 5.228 | 5.246 | 6.217 | 4.490 |
| Ca | - | - | - | - | - | - | 0.058 | - | - | - | - | - | - | - |
| | | | | | | | | | | | | | | |
| Z | 8.000 | 8.000 | 8.000 | 8.000 | 8.000 | 8.000 | 8.000 | 8.000 | 8.000 | 8.000 | 8.000 | 8.000 | 8.000 | 8.000 |
| Y | 11.771 | 11.724 | 11.847 | 11.803 | 11.757 | 11.800 | 11.777 | 11.811 | 11.769 | 11.712 | 11.893 | 11.851 | 11.871 | 11.863 |

| | Gray banded marble | | | | | | | Massive marble w |
|---|---|---|---|---|---|---|---|---|
| | Stelae 29 | | Aymavilles quarry | | | Stelae 6 | | |
| ANAL. NR. | Phl 1 | Phl 2 | Phl 3 | Phl 4 | Grt 1 | Grt 2 | Grt 3 | Grt 4 |
| $SiO_2$ | 46.64 | 46.44 | 46.05 | 45.34 | 37.36 | 37.49 | 37.25 | 37.46 |
| $TiO_2$ | bdl | bdl | bdl | bdl | bdl | bdl | bdl | bdl |
| $Al_2O_3$ | 12.14 | 12.14 | 12.14 | 13.32 | 20.44 | 20.87 | 20.82 | 20.82 |
| FeO | bdl | bdl | bdl | bdl | 16.66 | 17.90 | 19.41 | 18.33 |
| MnO | bdl | bdl | bdl | bdl | 16.44 | 14.36 | 12.44 | 13.22 |
| MgO | 28.10 | 28.02 | 28.30 | 27.79 | 0.34 | 0.46 | 0.50 | 0.81 |
| CaO | bdl | bdl | 0.37 | bdl | 8.85 | 9.76 | 9.54 | 9.63 |
| $Na_2O$ | bdl | bdl | 0.38 | bdl | bdl | bdl | bdl | bdl |
| $K_2O$ | 8.78 | 8.77 | 8.00 | 8.67 | bdl | bdl | bdl | bdl |
| ***** | ***** | ***** | ***** | ***** | ***** | ***** | ***** | ***** |
| Total | 95.67 | 95.37 | 95.26 | 95.11 | 100.08 | 100.85 | 99.98 | 100.28 |
| Si | 6.325 | 6.319 | 6.268 | 6.189 | 3.008 | 2.990 | 2.995 | 2.996 |
| Al IV | 1.675 | 1.681 | 1.732 | 1.811 | - | 0.010 | 0.005 | 0.004 |
| Al VI | 0.265 | 0.264 | 0.216 | 0.331 | 1.939 | 1.951 | 1.967 | 1.958 |
| Ti | - | - | - | - | - | - | - | - |
| $Fe^{3+}$ | - | - | - | - | 0.059 | 0.051 | 0.034 | 0.043 |
| $Fe^{2+}$ | - | - | - | - | 1.062 | 1.143 | 1.270 | 1.183 |
| Mn | - | - | - | - | 1.121 | 0.970 | 0.848 | 0.896 |
| Mg | 5.680 | 5.683 | 5.742 | 5.655 | 0.041 | 0.055 | 0.061 | 0.097 |
| Ca | - | - | 0.054 | - | 0.763 | 0.834 | 0.822 | 0.825 |
| Na | - | - | 0.101 | - | - | - | - | - |
| K | 1.519 | 1.523 | 1.390 | 1.510 | - | - | - | - |
| Z | 8.000 | 8.000 | 8.000 | 8.000 | 3.008 | 3.000 | 3.000 | 3.000 |
| Y | 5.945 | 5.947 | 5.958 | 5.985 | 1.998 | 2.002 | 2.001 | 2.001 |
| X | 1.519 | 1.523 | 1.545 | 1.510 | 2.987 | 3.001 | 3.001 | 3.001 |

vith silicate layers

| Stelae 40 | | | |
|---|---|---|---|
| Amph 1 | Amph 2 | Amph 3 | Amph 4 |
| 52.65 | 53.90 | 53.15 | 53.95 |
| bdl | bdl | bdl | bdl |
| 5.01 | 3.85 | 4.82 | 2.61 |
| 16.26 | 15.57 | 15.63 | 15.68 |
| bdl | bdl | bdl | bdl |
| 13.10 | 13.87 | 13.44 | 14.23 |
| 11.15 | 11.60 | 11.17 | 12.28 |
| 1.00 | 1.05 | 1.17 | 0.51 |
| bdl | bdl | bdl | bdl |
| ***** | ***** | ***** | ***** |
| 99.16 | 99.83 | 99.40 | 99.28 |
| | | | |
| 7.559 | 7.665 | 7.591 | 7.731 |
| 0.441 | 0.335 | 0.409 | 0.269 |
| | | | |
| 0.406 | 0.310 | 0.403 | 0.172 |
| - | - | - | - |
| - | - | - | - |
| | | | |
| 1.953 | 1.852 | 1.867 | 1.880 |
| - | - | - | - |
| 2.804 | 2.940 | 2.862 | 3.040 |
| | | | |
| 1.716 | 1.767 | 1.710 | 1.886 |
| 0.278 | 0.288 | 0.324 | 0.143 |
| - | - | - | - |